Journal of Economic Dynamics & Control 119 (2020) 103979

Contents lists available at ScienceDirect

Journal of Economic Dynamics & Control

journal homepage: www.elsevier.com/locate/jedc

European spreads at the interest rate lower bound☆

Laura Coroneo[a], Sergio Pastorello[b,*]

[a] Department of Economics and Related Studies, University of York, York, YO10 5DD, United Kingdom
[b] University of Bologna, Dipartimento di Scienze Economiche, Piazza Scaravilli 2, Bologna 40126, Italy

ARTICLE INFO

Article history:
Received 30 September 2019
Revised 17 August 2020
Accepted 21 August 2020
Available online 28 August 2020

JEL classification:
E43
E44
E52
G12

Keywords:
Lower bound
Sovereign risk
Shadow rate term structure model

ABSTRACT

This paper analyzes the effect of the interest rate lower bound on long-term sovereign bond spreads in the euro area. We specify a joint shadow rate term structure model for the risk-free, the German, and the Italian sovereign yield curves. In our model, the behavior of long-term spreads becomes strongly nonlinear in the underlying factors when interest rates are close to the lower bound, which occurs in the data since the beginning of 2012. We fit the model via Quasi-Maximum Likelihood and show three consequences of the nonlinear behavior of sovereign spreads: (i) they are asymmetrically distributed, (ii) they are affected by (possibly exogenous) changes in the lower bound, and (iii) they become less informative about sovereign risk than when interest rates are far from the lower bound. Shadow spreads, however, still provide reliable information.

1. Introduction

Long term sovereign bond spreads are closely monitored by financial markets, central banks, and governments as a reference measure of sovereign risk. According to standard finance theory, long-term rates are determined by the current and expected future short-term rates plus a risk premium, i.e. by the current forward curve. Consequently, a lower bound constraining forward sovereign rates will also affect long-term sovereign rates, as well as long-term sovereign bond spreads.

The existence of a lower bound on interest rates can be justified both theoretically and empirically. Black (1995) was the first to observe that interest rates cannot decrease below the opportunity cost of holding currency, which represents a lower bound on interest rates. This implies that standard Gaussian affine dynamic term structure models are misspecified when observed yields are close to the bound, because they assign a large probability to rates below it. Empirically, this situation has become relevant in several countries: in Japan since the late 1990s, in the US since 2009, and in the euro area since 2012.

Several authors have suggested that shadow rate term structure models can be used to enforce a lower bound on interest rates; see Krippner (2015), Wu and Xia (2016), and Christensen and Rudebusch (2014). These papers show that shadow rate term structure models fit observed yields better than Gaussian affine dynamic term structure models, and offer several advantages in periods when rates are constrained from below. Some efforts have also been devoted to highlighting the implications of the lower bound on long-term yields. In the context of a shadow rate term structure model, Krippner (2015) and

☆ Laura Coroneo gratefully acknowledges the support of the ESRC grant ES/K001345/1.
* Corresponding author.
E-mail addresses: laura.coroneo@york.ac.uk (L. Coroneo), sergio.pastorello@unibo.it (S. Pastorello).

https://doi.org/10.1016/j.jedc.2020.103979
0165-1889/

Bauer and Rudebusch (2016) measure how tightly the zero lower bound constrains the entire term structure of interest rates using the zero lower bound wedge, which is defined as the difference between the 10-year yield and the corresponding shadow yield, i.e. the yield that would be observed if interest rates were not constrained. Ruge-Murcia (2006) shows that, at the lower bound, long-term rates respond asymmetrically to changes in the short-term rate, and by less than predicted by a Gaussian affine dynamic term structure model. Swanson and Williams (2014a) measure the tightness of the zero lower bound on medium and long-term interest rates using the interest rate sensitivity to macroeconomic news. However, it is not clear what these results imply for the behavior of sovereign spreads.

In this paper, we focus on the effect of the interest rate lower bound on long-term sovereign bond spreads. To this end, we specify a joint shadow rate term structure model for the risk-free, the German, and the Italian yield curves in a monetary union. Our model allows for common and country-specific factors, and also for a time varying lower bound. In this framework, observed sovereign spreads can be decomposed in two components: the shadow spread and the spread wedge. The shadow spread is linear in the state variables and represents the unconstrained sovereign spread, i.e. the sovereign spread that we would observe in the absence of a lower bound, or if interest rates were far from it. The spread wedge instead captures the nonlinearities that arise when short-term rates are close to the lower bound, and it measures the extent to which the lower bound is distorting the observed sovereign spread. Its size depends on the distance of the forward curves of the two countries from the lower bound, and also on the volatilities of shadow rates under the risk-neutral probability measure. As the forward curve of one of the two countries approaches the lower bound, a larger proportion of the observed spread is determined by the spread wedge and, as a consequence, the observed spread loses its informative content as a measure of sovereign risk.

The sovereign debt crisis that affected peripheral European countries and threatened the sustainability of the euro zone, accompanied by the decline in euro area interest rates towards a lower bound, offers the ideal setup to assess the relevance of the nonlinearities in sovereign spreads that arise due to the presence of an interest rate lower bound. In this period, Italy – the third largest economy in the euro area – experienced increased turmoil in its sovereign bond market. The Italian debt-to-GDP ratio is the second highest in Europe, and the Italian absolute debt is higher than that of Greece, Ireland, Portugal, and Spain combined. Therefore, because of the size of Italian debt, the turmoil in the Italian sovereign market was concerning for its potential effect on the euro zone as a whole. For these reasons, during the sovereign debt crisis, the spread between the 10-year Italian bond and the 10-year German bond became a key indicator of the health of the euro zone. In addition, as noted in Lemke and Vladu (2017), from the onset of the euro zone crisis, German government bonds experienced safe-haven flows that pushed German yields below risk-free rates. Accordingly, our analysis focuses on long-term Italian sovereign spreads with respect to both German and euro area risk-free rates.

We estimate our joint shadow rate term structure model by quasi-maximum likelihood and the Extended Kalman filter, using zero-coupon rates computed from euro area overnight index swaps (OIS), and German and Italian Treasury yields for the period January 2001 to January 2020. As in recent studies on euro area yield curves (see Kortela, 2016; Lemke and Vladu, 2017; Pericoli and Taboga, 2015), we use OIS rates as a proxy for risk-free rates in the euro area. Thus the spread between the yield of a country with respect to the OIS yield with the same maturity can be interpreted as the net effect of its sovereign risk and safety premium. We specify a model with five factors, two of which are common to the three curves, one specific to Germany, and two specific to Italy.

Our results show that spread wedges became non-negligible since 2012, indicating the presence of strong nonlinearities in the behavior of long-term sovereign spreads at the interest rate lower bound. In particular, we find that in 2012 the spread wedge component in the 10-year Italian spreads with respect to OIS and German rates reached, respectively, -42 and -53 basis points, indicating that in this period the interest rate lower bound was constraining OIS and German rates more than the Italian ones, and that in the absence of a lower bound the 10-year Italian spreads would have been higher.

Our focus on the behavior of sovereign spreads when interest rates are at or near the lower bound is novel and enables us to highlight three important implications. First, as interest rates approach their lower bound, the conditional distribution of future spreads becomes skewed. For the Italian spreads with respect to German and OIS rates, we find that the distributions of future spreads are skewed to the right and that the degree of skewness decreases with the maturity, but is still substantial even for the 10-year spreads at a 1-year horizon. Second, spreads depend on the distance from the lower bound. This implies that an exogenous change in the lower bound affects the observed spread even if the sovereign risk does not change. More specifically, our results indicate that an exogenous decrease of the lower bound by 20 basis points increases the 10-year Italian spreads with respect to German and OIS rates by as much as 7 basis points. Third, at or near the interest rate lower bound, the observed spread loses its informative content as a measure of sovereign risk but the shadow spread does not. In particular, we find that the relation between the 10-year sovereign Credit Default Swaps (CDS) spread between Italy and Germany and the corresponding observed 10-year sovereign spread broke down because of a structural break around late 2011/early 2012, when the German forward curve approached the lower bound. On the contrary, the relation between the 10-year sovereign CDS spread and the 10-year sovereign shadow spread remained stable over the entire sample.

The paper is organized as follows. Section 2 provides a review of the related literature. Section 3 describes the joint shadow rate term structure model and Section 4 derives sovereign shadow spreads. Section 5 describes the data and performs some preliminary analyses. Section 6 describes the estimation methodology and the identification scheme. Section 7 describes the results, and Section 8 concludes.

2. Related literature

The idea of using a shadow rate to enforce a lower bound in interest rates was introduced by Black (1995), who noticed that interest rates cannot decrease below the opportunity cost of holding currency. As Japanese interest rates approached the lower bound in the late 1990s, researchers faced the computational challenge of estimating a term structure model that did not allow for a closed form solution. The two most notable examples are Ichiue and Ueno (2007) and Kim and Singleton (2012), who estimate a two-factor shadow rate term structure model using numerical approximation techniques. It was only when US interest rates reached the lower bound in 2008 that closed form approximations were developed by Krippner (2015), Wu and Xia (2016), and Christensen and Rudebusch (2014). The main difference between the three approximations lies in the specification of the shadow rate model used. In this paper, we use the approximation proposed by Wu and Xia (2016), which directly applies to a discrete time shadow rate term structure model, to estimate a multi-country shadow rate term structure model.

Closed form approximations made shadow rate term structure models tractable and allowed them to become suitable for policy analysis. In particular, following the suggestions of Wu and Xia (2016), Krippner (2013), and Bullard (2012), the shadow short rate became a popular measure of the stance of monetary policy at the interest rate lower bound, often used to replace the policy rate in structural macro models. As noted by Christensen and Rudebusch (2014) and Krippner (2020), shadow short rate estimates depend on the model specification and the model fit, but there is an agreement in the literature that different estimates are highly correlated (see Christensen and Rudebusch, 2014; Krippner, 2020; Wu and Xia, 2016). Shadow rate term structure models also provide more robust indicators such as the expected time to lift-off and the lower bound wedge. The expected time to lift-off, introduced by Wu and Xia (2016) and Krippner (2015), denotes the market-implied expected future date at which the short rate will lift off from the lower bound, while the lower bound wedge proposed by Krippner (2015) and Bauer and Rudebusch (2016) reflects the asymmetry induced by the lower bound on the distribution of future short rates, and hence reveals the relative tightness of the lower bound constraint. These measures are more robust than the shadow short rate because they exploit more information on long-term interest rates. In addition, as shown by Krippner (2015) and Bauer and Rudebusch (2016), these two measures are also highly correlated. Our paper introduces the sovereign spread wedge, which generalizes the interest rate lower bound wedge to long-term sovereign spreads, and measures how tightly the lower bound constrains long-term sovereign spreads.

Shadow rate term structure models usually assume that the lower bound is constant over time; its value is either fixed *a priori*, calibrated or estimated. This assumption seems appropriate for Japanese yields (see Christensen and Rudebusch, 2014; Ichiue and Ueno, 2007; Kim and Singleton, 2012; Krippner, 2013), US yields (see Bauer and Rudebusch, 2016; Christensen and Rudebusch, 2016; Kim and Priebsch, 2013; Krippner, 2012; Wu and Xia, 2016), and UK yields (see Carriero et al., 2018). However, the assumption of a constant lower bound is rejected for euro area yields by Lemke and Vladu (2017); in addition, Kortela (2016) and Wu and Xia (2020) find that a time-varying lower bound is better suited for European yields. Accordingly, we assume that the lower bound depends on the short-term risk-free rate for reserves at the European Central Bank (ECB) and on a time-varying parameter.

Multi-country affine term structure models have been classified by Egorov et al. (2011), and they are extensively used to investigate the interactions between domestic and foreign yield curves. However, the literature on shadow rate term structure models focuses exclusively on single yield curve settings, mainly because shadow rate models are computationally more intensive than standard affine ones. Carriero et al. (2018) and Dawachter et al. (2016) estimate joint shadow rate models imposing the lower bound constraint only on one yield curve. To the best of our knowledge, our paper is the first study of a shadow rate term structure model with lower-bound constrains on multiple yield curves. Our setup is a multi-country but single-currency model. This implies that, given that the lower bound represents the opportunity cost of holding currency, our model has a single lower bound that represents the opportunity cost of holding euros.

A large literature, starting with Edwards (1984), investigates the determinants of sovereign risk using sovereign spreads, see e.g. Alesina et al. (1992), and Borri and Verdelhan (2009). With the inception of the euro and, especially, with the European debt crisis, this literature has focused on the determinants of European sovereign spreads, see e.g. Manganelli and Wolswijk (2009), Beirne and Fratzscher (2013), and Monfort and Renne (2013). A common denominator of these works is that they use sovereign spreads as a proxy for sovereign risk, due to the common assumption that any nonlinearity induced by the interest rate lower bound is negligible for long-term spreads. Our results indicate that this assumption does not hold. In particular, we show that, when short-term risk-free rates in the euro area are close to the lower bound, the observed sovereign spreads become less informative about the sovereign risk, as a non-linear component caused by the lower bound emerges.

3. A joint shadow rate term structure model for yield curves in the euro area

3.1. Setup

We model the joint dynamics of the risk-free, the German, and the Italian yield curves using a nonlinear model with common and country-specific latent factors evolving according to linear Gaussian dynamics. Shadow interest rates are affine in the state variables, but observed rates are bounded by a time-varying exogenous lower bound. In this section, we describe each point in detail.

We assume that the shadow risk-free short-term interest rate s_t^0 is an affine function of n_0 common factors $\mathbf{x}_t^0$ related to the common monetary policy. We also assume that the German and the Italian shadow short-term interest rates, s_t^i, $i = GE, IT$, are affine functions of both the common factors $\mathbf{x}_t^0$ and of n_i country-specific factors $\mathbf{x}_t^i$, driven by credit quality or liquidity. Let $n = n_0 + n_{GE} + n_{IT}$, and denote the full $n \times 1$ vector of state variables as

$$\mathbf{x}_t = (\mathbf{x}_t^{0\prime}, \mathbf{x}_t^{GE\prime}, \mathbf{x}_t^{IT\prime})'.$$

Shadow rates can then be expressed as[1]

$$s_t^i = \delta_0^i + \delta_1^{i\prime}\mathbf{x}_t, \quad i = 0, GE, IT, \tag{1}$$

where:

$$\delta_1^0 = \begin{pmatrix} \delta_1^{0,0} \\ \mathbf{0}_{n_{GE}\times 1} \\ \mathbf{0}_{n_{IT}\times 1} \end{pmatrix}, \quad \delta_1^{GE} = \begin{pmatrix} \delta_1^{GE,0} \\ \delta_1^{GE,GE} \\ \mathbf{0}_{n_{IT}\times 1} \end{pmatrix}, \quad \delta_1^{IT} = \begin{pmatrix} \delta_1^{IT,0} \\ \mathbf{0}_{n_{GE}\times 1} \\ \delta_1^{IT,IT} \end{pmatrix}.$$

We assume that the state variables follow a first order vector autoregressive process under the physical measure $\mathbb{P}$

$$\mathbf{x}_{t+1} = \mu + \mathbf{\Phi}\mathbf{x}_t + \mathbf{\Gamma}\varepsilon_{t+1}, \tag{2}$$

where $\varepsilon_{t+1} \overset{\mathbb{P}}{\sim} \mathcal{N}_{IID}(\mathbf{0}, \mathbf{I}_n)$ and $\mathbf{\Gamma}$ is a lower triangular matrix. We also assume that there exists a risk-neutral probability measure $\mathbb{Q}$ which prices all financial assets and under which the risk factors follow a first order Gaussian vector autoregression

$$\mathbf{x}_{t+1} = \mu^{\mathbb{Q}} + \mathbf{\Phi}^{\mathbb{Q}}\mathbf{x}_t + \mathbf{\Gamma}\varepsilon_{t+1}^{\mathbb{Q}}, \tag{3}$$

where $\varepsilon_{t+1}^{\mathbb{Q}} \overset{\mathbb{Q}}{\sim} \mathcal{N}_{IID}(\mathbf{0}, \mathbf{I}_n)$. To ensure that $\mathbf{x}_t^{GE}$ and $\mathbf{x}_t^{IT}$ are country-specific factors, we impose that the $(n_{GE} + n_{IT}) \times (n_{GE} + n_{IT})$ lower right block of $\mathbf{\Phi}^{\mathbb{Q}}$ is block-diagonal.

Notice that jointly modeling euro area risk-free rates alongside German and Italian yields allows us to interpret country factors as capturing the net effect of the credit risk premium and the convenience yield of holding bonds. This approach also allows us to take into account possible spillovers from $\mathbf{x}_t^{IT}$ to $\mathbf{x}_t^{GE}$, as the matrix $\mathbf{\Phi}$ in (2) is unrestricted.

Under the no-arbitrage condition, the price $p_{t,\tau}^i$ of a zero-coupon bond with τ months to maturity in country i can be expressed as

$$p_{t,\tau}^i = E_t^{\mathbb{Q}}\left[\exp\left(-\sum_{j=0}^{\tau-1} r_{t+j}^i\right)\right], \quad i = 0, GE, IT \tag{4}$$

where r_t^i is the short-term interest rate in country i.

The lower bound on interest rates can be enforced by allowing the short-term interest rate to be equal to the shadow short rate only when the latter is above the lower bound, and otherwise equal to the lower bound:

$$r_t^i = \max(s_t^i, \underline{r}_t), \quad i = 0, GE, IT. \tag{5}$$

This is the shadow rate term structure model first introduced by Black (1995), in which the idea is that short-term interest rates are bounded below due to the option to convert to currency. As a result of this option, all term rates are bounded, but do not have a reflecting boundary condition, as opposed to affine models with factors that follow square-root processes or quadratic Gaussian models. An appealing feature of the shadow rate term structure model is that, when short-term interest rates are far from the lower bound, interest rates behave as in a Gaussian affine term structure model. Notice that $\underline{r}_t$ can be slightly positive, zero or negative as it represents the return of holding euros (net of the costs associated with storing, insuring, and transferring large amounts of currency), which is common across the three yield curves.

3.2. Solution

The assumption in (5) implies that yields are nonlinear in the state variables and do not have an analytical expression. Denote by $f_{t,\tau}^i$ the time t one period forward rate in country i for a loan starting at $t + \tau$. Forward rates and bond yields are related by the following general property:

$$y_{t,\tau}^i = \frac{1}{\tau}\sum_{j=0}^{\tau-1} f_{t,j}^i, \quad i = 0, GE, IT. \tag{6}$$

[1] In what follows, we refer to the risk-free yield curve as the yield curve of country 0.

Wu and Xia (2016) show that, under (1)–(5), the forward rate $f^i_{t,\tau}$ is approximately equal to[2]

$$f^i_{t,\tau} \approx \underline{r}_t + \sigma^i_\tau g\left(\frac{a^i_\tau + \mathbf{b}^{i\prime}_\tau \mathbf{x}_t - \underline{r}_t}{\sigma^i_\tau}\right), \quad i = 0, GE, IT, \tag{7}$$

where:

$$\begin{aligned}
&g(z) = zN(z) + n(z),\\
&\mathbf{b}^i_\tau = \left[(\boldsymbol{\Phi}^{\mathbb{Q}})^\tau\right]' \delta^i_1,\\
&a^i_\tau = \delta^i_0 + \left(\sum_{j=0}^{\tau-1} \mathbf{b}^i_j\right)' \mu^{\mathbb{Q}} - \frac{1}{2}\left(\sum_{j=0}^{\tau-1} \mathbf{b}^i_j\right)' \boldsymbol{\Gamma}\boldsymbol{\Gamma}' \left(\sum_{j=0}^{\tau-1} \mathbf{b}^i_j\right),\\
&\left(\sigma^i_\tau\right)^2 = \sum_{j=0}^{\tau-1} \mathbf{b}^{i\prime}_j \boldsymbol{\Gamma}\boldsymbol{\Gamma}' \mathbf{b}^i_j,
\end{aligned} \tag{8}$$

with $N(\cdot)$ and $n(\cdot)$ denoting the cdf and the pdf of the standard normal distribution, respectively. The approximation in (7) only holds for $\tau \geq 1$. For $\tau = 0$, given $f^i_{t,0} = r^i_t$, (5) implies

$$f^i_{t,0} = \underline{r}_t + \max(0, \delta^i_0 + \delta^{i\prime}_1 \mathbf{x}_t - \underline{r}_t), \quad i = 0, GE, IT. \tag{9}$$

Plugging the approximate expressions for the forward rates in (7) and (9) into (6), we can construct an approximation for the yields $y^i_{t,\tau}$:

$$y^i_{t,\tau} = \underline{r}_t + \frac{1}{\tau}\left[\max(0, \delta^i_0 + \delta^{i\prime}_1 \mathbf{x}_t - \underline{r}_t) + \sum_{j=1}^{\tau-1} \sigma^i_j g\left(\frac{a^i_j + \mathbf{b}^{i\prime}_j \mathbf{x}_t - \underline{r}_t}{\sigma^i_j}\right)\right] = h^i_\tau(\mathbf{x}_t) \tag{10}$$

for $i = 0, GE, IT$.

3.3. Shadow yield curve

The short rate Eq. (5) introduces nonlinearity into a term structure model with linear Gaussian dynamics and, as a consequence, yields are nonlinear in the state variables. However, the model enables us to compute shadow yields, i.e. the component in interest rates that is always linear in the state variables.

The short rate Eq. (5) can be written as

$$r^i_t = f^i_{t,0} = s^i_t + \max(\underline{r}_t - s^i_t, 0), \quad i = 0, GE, IT, \tag{11}$$

where s^i_t is linear in the state variables, see (1), and $\max(\underline{r}_t - s^i_t, 0)$ represents the option value of cash (see Krippner, 2015). A similar decomposition for forward rates with $\tau \geq 1$ can be derived using the approximation in (7). In particular, if we define shadow forward rates $\tilde{f}^i_{t,\tau}$ as

$$\tilde{f}^i_{t,\tau} = a^i_\tau + \mathbf{b}^{i\prime}_\tau \mathbf{x}_t, \quad i = 0, GE, IT$$

we can rewrite (7) as:

$$f^i_{t,\tau} = \tilde{f}^i_{t,\tau} + z^i_{t,\tau}, \quad i = 0, GE, IT, \tag{12}$$

where the option value of cash $z^i_{t,\tau}$ is given by

$$z^i_{t,\tau} = \left(\underline{r}_t - \tilde{f}^i_{t,\tau}\right)\left[1 - N\left(\frac{\tilde{f}^i_{t,\tau} - \underline{r}_t}{\sigma^i_\tau}\right)\right] + \sigma^i_\tau n\left(\frac{\tilde{f}^i_{t,\tau} - \underline{r}_t}{\sigma^i_\tau}\right) > 0, \quad i = 0, GE, IT. \tag{13}$$

As shown in the top plot in Fig. 1, the option value of cash $z^i_{t,\tau}$ depends on both the distance of the shadow forward rate from the lower bound $(\tilde{f}^i_{t,\tau} - \underline{r}_t)$ and on the volatility of the τ-period shadow rate of country i under the risk-neutral distribution, σ^i_τ defined in (8). The option value of cash is large and positive when shadow forward rates are close to or below the lower bound, otherwise it is negligible. In addition, the larger the volatilities of shadow rates under the risk-neutral measure, the larger the option value of cash.

Given that the option value of cash is always greater than zero, Eq. (12) implies that the observed forward rate is always greater than the corresponding shadow forward rate, i.e. $f^i_{t,\tau} \geq \tilde{f}^i_{t,\tau}$. The difference between the two is larger (i) the closer

[2] To price forward rates, we assume that $\underline{r}_t$ is exogenous to the model, as agents allow for future revisions to the lower bound, but ignore this uncertainty when pricing bonds and swaps. This assumption is in line with the anticipated utility approach of Kreps (1998) that has been shown to be a good approximation of agents' behavior, see Cogley and Sargent (2008), and that is frequently used in the asset pricing literature with time-varying parameters, see Orphanides and Wei (2012).

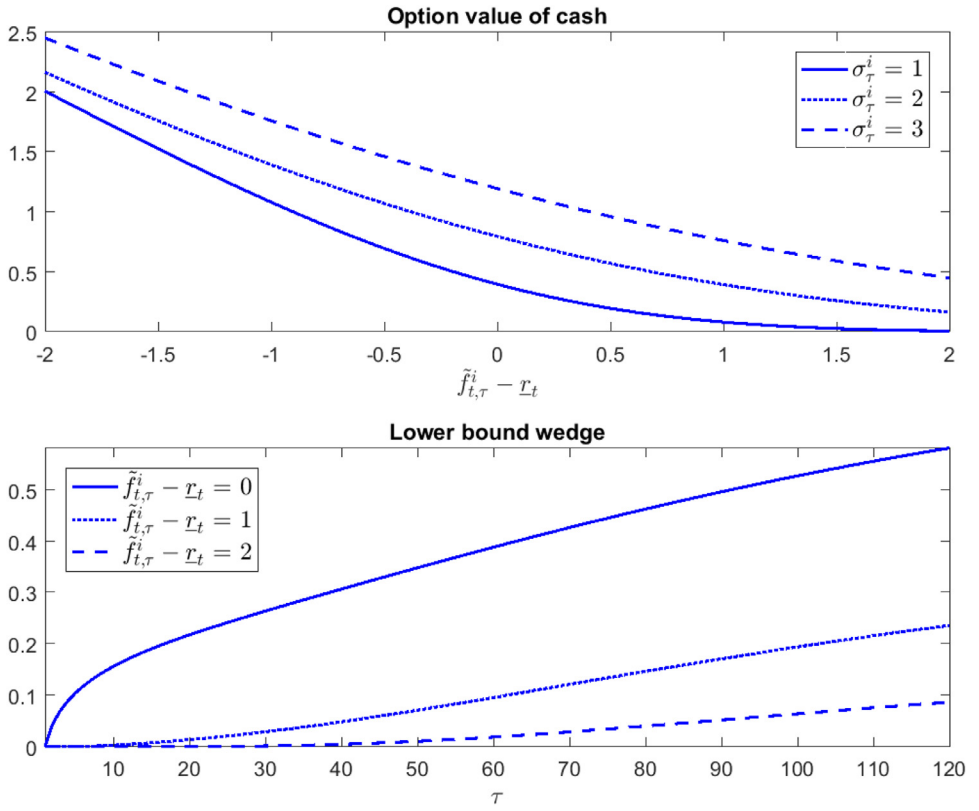

Fig. 1. Option value of cash and lower bound wedge. The top figure plots the option value of cash $z^i_{t,\tau}$ defined in (13) as a function of the distance of the shadow forward rate from the lower bound $\tilde{f}^i_{t,\tau} - \underline{r}_t$ and for different values of σ^i_τ, the volatilities of shadow rates under the risk-neutral measure. The bottom figure illustrates the lower bound wedge $Z^i_{t,\tau}$ defined in (17) as a function of the maturity τ and for different values of the distance of the shadow forward rate from the lower bound $\tilde{f}^i_{t,\tau} - \underline{r}_t$. The lower bound wedges are computed assuming a flat forward curve, and a curve for the volatilities of shadow rates that matches the curve estimated on OIS rates, as reported in Fig. 6. All values are in percentage points.

the observed short-term rate is to the lower bound and (*ii*) the larger the volatilities of shadow rates. The reason for (*i*) is that close to the lower bound, agents understand that the range of possible realizations of future short-term interest rates is larger above than below the current level, and therefore the distribution of future rates is skewed to the right, which in turn implies $f^i_{t,\tau} = E^{\mathbb{Q}}(r_{t+\tau}|\mathbf{x}_t) > E^{\mathbb{Q}}(s_{t+\tau}|\mathbf{x}_t) = \tilde{f}^i_{t,\tau}$. The reason for (*ii*) is that the larger the volatilities of shadow rates, the more likely it is that the range of possible values of future shadow short rates includes values that are below the lower bound. This again implies a large difference between expected future short rates and expected future shadow rates (under the $\mathbb{Q}$ distribution), and a larger option value of cash.

The option value of cash generates a wedge between observed and shadow yields at any maturity. To see this, substitute the decompositions (11) and (12) in (6), to obtain:

$$y^i_{t,\tau} = \tilde{y}^i_{t,\tau} + Z^i_{t,\tau}, \quad i = 0, GE, IT, \tag{14}$$

where the shadow yield $\tilde{y}^i_{t,\tau}$ is given by

$$\tilde{y}^i_{t,\tau} = \frac{1}{\tau}\sum_{j=0}^{\tau-1}\tilde{f}^i_{t,\tau} = \frac{1}{\tau}\left[\delta^i_0 + \delta^{i\prime}_1\mathbf{x}_t + \sum_{j=1}^{\tau-1}\left(a^i_j + \mathbf{b}^{i\prime}_j\mathbf{x}_t\right)\right] = A^i_\tau + \mathbf{B}^{i\prime}_\tau\mathbf{x}_t, \quad i = 0, GE, IT, \tag{15}$$

with

$$A^i_\tau = \frac{1}{\tau}\left(\delta^i_0 + \sum_{j=1}^{\tau-1}a^i_j\right), \quad \mathbf{B}^i_\tau = \frac{1}{\tau}\left(\delta^i_1 + \sum_{j=1}^{\tau-1}\mathbf{b}^i_j\right), \quad i = 0, GE, IT, \tag{16}$$

and the lower bound wedge $Z^i_{t,\tau}$ is given by

$$Z^i_{t,\tau} = \frac{1}{\tau}\left[\max(\underline{r}_t - s^i_t, 0) + \sum_{j=1}^{\tau-1}z^i_{t,j}\right] > 0, \quad i = 0, GE, IT. \tag{17}$$

Eq. (14) shows that shadow rate term structure models enable us to decompose observed yields in two components: the shadow yield $\tilde{y}^i_{t,\tau}$ (which is linear in the state variables) and the lower bound wedge $Z^i_{t,\tau}$ (which is the cumulative sum of the option values of cash). Thus, observed yields are always greater than the corresponding shadow yields, i.e. $y^i_{t,\tau} \geq \tilde{y}^i_{t,\tau}$. The difference among the two is the lower bound wedge generated by the nonlinearities that arise at the lower bound and that can be seen as a measure of how tightly the lower bound constrains the observed yield (see Bauer and Rudebusch, 2016; Krippner, 2015). As yields move away from the lower bound, the wedge becomes negligible and observed yields approach their shadow counterparts.

The bottom plot of Fig. 1 reports the lower bound wedge as a function of the maturity of the bond, for different values of the distance of the shadow forward rate from the lower bound and for a flat forward curve. As expected, the lower bound wedge is larger when the shadow forward rate is closer to the lower bound.

4. Sovereign spreads at the interest rate lower bound

We define the sovereign spread between yields of countries i and j with maturity τ as $\Delta^{i,j}_{t,\tau} = y^i_{t,\tau} - y^j_{t,\tau}$. We then use (14) to decompose observed sovereign spreads as

$$\Delta^{i,j}_{t,\tau} = \tilde{\Delta}^{i,j}_{t,\tau} + Z^{i,j}_{t,\tau}, \quad i, j = 0, GE, IT, \tag{18}$$

where the shadow sovereign spread $\tilde{\Delta}^{i,j}_{t,\tau}$ is given by

$$\tilde{\Delta}^{i,j}_{t,\tau} = \tilde{y}^i_{t,\tau} - \tilde{y}^j_{t,\tau}, \tag{19}$$

and the sovereign spread wedge $Z^{i,j}_{t,\tau}$ is

$$Z^{i,j}_{t,\tau} = Z^i_{t,\tau} - Z^j_{t,\tau} = \frac{1}{\tau}\left[\max(\underline{r}_t - s^i_t, 0) - \max(\underline{r}_t - s^j_t, 0) + \sum_{s=1}^{\tau-1}(z^i_{t,s} - z^j_{t,s})\right]. \tag{20}$$

Eq. (18) shows that also the observed sovereign spread can be decomposed in two components: the shadow spread $\tilde{\Delta}^{i,j}_{t,\tau}$, which is linear in the state variables, and the sovereign spread wedge $Z^{ij}_{t,\tau}$, which measures the nonlinearities that arise at the lower bound, i.e. by how much the lower bound is constraining the observed sovereign spread. The latter depends on the distance of each of the two forward curves from the lower bound and on the volatilities of shadow rates in each country under $\mathbb{Q}$.

The sovereign spread wedge is the difference between expected future short-term spreads and shadow spreads, both under $\mathbb{Q}$. If for one country the short-term rate approaches the lower bound, agents understand that the range of possible values of future short-term interest rates in this country is larger above than below the current short-term rate. This implies that expected future short-term spreads are above (if the constrained country is i) or below (if the constrained country is j) the current short-term spread.

Let us assume for simplicity that the volatilities of the shadow rates under the risk-neutral distribution are the same for both countries. In this case, if the forward rates of the two countries are far from the lower bound, the sovereign spread wedge is negligible and the observed spread is close to the shadow spread. However, if at least one of the two forward curves is close to the lower bound, the sovereign spread wedge is non-negligible and the observed spread is different from the shadow spread. The sign of the sovereign spread wedge depends on which of the two forward curves is closer to the lower bound, and thus more constrained by it.

To further simplify the discussion, let us consider $\Delta^{i,0}_{t,\tau}$, i.e. the spread between the yield with maturity τ of country i with respect to the risk-free yield with the same maturity. In the presence of sovereign risk, the yield curve of country i is above the risk-free yield curve and, as rates decline towards the lower bound, the risk-free yield curve becomes more constrained by it, i.e. $Z^0_{t,\tau} \geq Z^i_{t,\tau}$. This implies that the sovereign spread wedge is negative, i.e. $Z^{i0}_{t,\tau} = Z^i_{t,\tau} - Z^0_{t,\tau} \leq 0$, and the observed spread is smaller than the shadow spread, i.e. $0 \leq \Delta^{i,0}_{t,\tau} = \tilde{\Delta}^{i,0}_{t,\tau} + Z^{i0}_{t,\tau} \leq \tilde{\Delta}^{i,0}_{t,\tau}$. The opposite happens in the presence of a convenience yield, because in this case the yield curve of country i is below the risk-free yield curve and, as rates decrease towards the lower bound, the yield curve of country i becomes more constrained by the bound than the risk-free yield curve, i.e $Z^i_{t,\tau} \geq Z^0_{t,\tau}$.

The consequence of Eq. (18) is that, as short-term rates approach the lower bound, the observed spread loses its informative content as a measure of sovereign risk. A decrease in the observed spread could be either due to a decrease of the shadow spread or to a decrease of the sovereign spread wedge. However, while changes in the shadow spread are solely determined by sovereign risk, changes in the sovereign spread wedge also depend on the distance of the two yield curves from the lower bound. For example, in the presence of sovereign risk, an exogenous decrease of the lower bound decreases the wedge on risk-free rates more than the one on the rates of country i, and thus increases the sovereign spread wedge. This also implies that the observed spread increases, even if the shadow spread and the sovereign risk are not affected. For this reason, when interest rates are constrained by the lower bound, the shadow spread is a more informative measure of the sovereign risk.

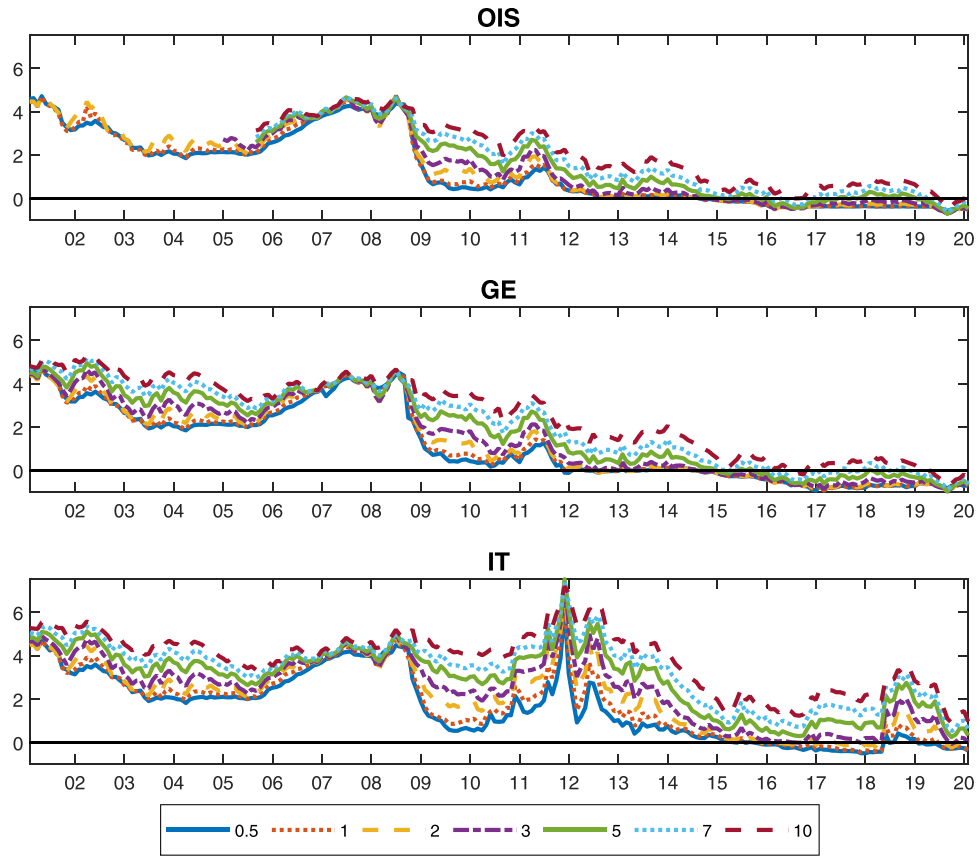

Fig. 2. Data. This figure reports end-of-month zero-coupon rates on OIS based on EONIA (top plot), German Treasury bonds (middle plot), and Italian Treasury bonds (bottom plot). The sample is January 2001 to January 2020 and the maturities are 6 months, 1, 2, 3, 5, 7 and 10 years.

5. Data and preliminary evidence

We use end-of-month zero-coupon rates on German and Italian Treasury bonds, and on OIS based on EONIA (the overnight unsecured interbank rate in the euro area). All data are provided by Datastream-Eikon and span the period January 2001 to January 2020 for maturities of 6 months, 1, 2, 3, 5, 7 and 10 years.[3]

To model the lower bound, we use the deposit facility rate of the Eurosystem. This is a monetary policy instrument under the direct control of the ECB, as it is the rate banks receive for depositing money with the central bank overnight. End-of-month data for the euro overnight interest rate is obtained from Datastream. In the last section of the paper, we relate spreads and shadow spreads to sovereign credit default swap (CDS) spreads. To this end, we use end-of-month data on 10-year Italian and German CDS spreads from Datastream. The first observation available for both CDS spreads is December 2007.

In Fig. 2 we plot the full dataset of yields used in the analysis. OIS, German, and Italian rates started with similar values at the outset of the sample but began to diverge in 2009. Italian rates started to increase in 2010 and spiked at the end of 2011, due to an increase in the sovereign risk premium. On the contrary, OIS and German rates steadily decreased towards zero. OIS short rates reached zero by mid-2012, but due to a number of reasons (flight to quality in the European bond market, use of German bonds as collateral for short-term borrowing in repo markets or as liquidity management instruments), German short rates already reached zero by the end of 2011. Indeed, Swanson and Williams (2014b) find that German short and medium rates have been significantly constrained by the lower bound since 2012. OIS and German short rates stayed at zero until mid-2014, when they turned negative. Italian short rates reached zero only at the beginning of 2015 and became negative at the end of the year. Fig. 2 also shows that all of the German and OIS yield curves are negative at the end of the sample. In this period, the term spread for OIS and German rates is much lower than the Italian one.

[3] OIS rates with maturity of 3 years are available from December 2004, and OIS rates with longer maturities are available from August 2005. German and Italian zero-coupon rates with maturity of 6 months are not available before 2007; for this maturity we use the zero-coupon rates provided by the Deutsche Bundesbank and the Italian Ministry of Economy and Finance up to December 2006.

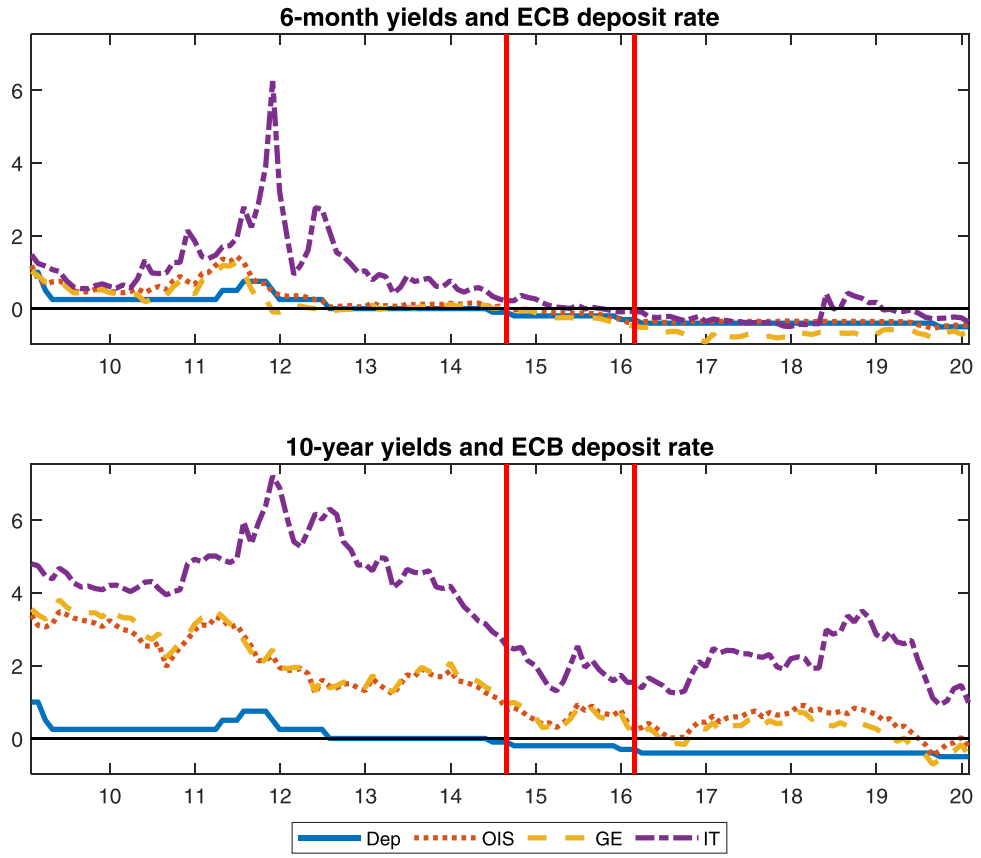

Fig. 3. Yields and ECB deposit rate. This figure reports the ECB deposit rate along with OIS, German and Italian yields with maturity of 6 months (top plot) and 10 years (bottom plot). The vertical lines denote August 2014 and February 2016.

5.1. Lower bound specification

The lower bound represents the return of holding euros (net of the costs associated with storing, insuring, and transferring large amounts of currency), which is common across the three yield curves. The behavior of yields in Fig. 2 highlights the need for a time-varying lower bound specification, as also noted by Lemke and Vladu (2017), Kortela (2016), and Wu and Xia (2020). To investigate the behavior of the lower bound, in Fig. 3 we plot the 6-month and the 10-year OIS, German, and Italian yields along with the deposit facility rate of the Eurosystem.

Fig. 3 shows that the 10-year rates are always above the ECB deposit rate. For 6-month rates, however, we can identify three subperiods. The first is up to August 2014, in which short-term rates are bounded from below either by zero or the deposit rate.[4] The second is from September 2014 to February 2016, when OIS and German rates turned negative. The last subperiod is from March 2016 to the end of the sample, when short-term OIS and German rates are negative and below the ECB deposit rate.[5] These three subperiods are highlighted with vertical lines in Fig. 3. Accordingly, we model the lower bound as follows:

$$\underline{r}_t = \min(0, d_t) + c_t, \tag{21}$$

where d_t is the ECB deposit rate and c_t is a coefficient that allows the lower bound to be different from zero or the deposit rate. This because, as noted by Lemke and Vladu (2017), the effective lower bound is the bound *perceived* by market participants and it can be different from zero or the deposit rate.

Fig. 4 reports the difference between daily 3-month rates and the minimum between the ECB deposit rate and zero. In the first part of the sample (up to August 2014), the value of this difference is mostly positive, indicating that interest rates are effectively constrained by a zero lower bound. In 2015, the figure shows that German rates are below the ECB deposit

[4] Lemke and Vladu (2017) find a significant change in the lower bound parameter in August 2014. Model estimates using only this date as a break for the lower bound parameter fit the data poorly at the end of the sample, indicating that an additional break is required.

[5] Preliminary results, available upon request, with an earlier date for the second break are similar to the ones presented in the paper, but allowing for a break later in the sample enables us to better fit the data.

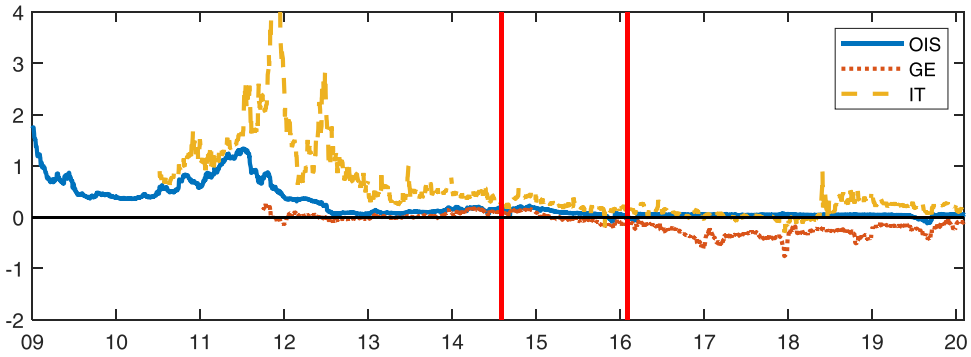

Fig. 4. Daily 3-month rates $-\min(0, d_t)$. This figure reports daily 3-month rates for OIS, German, and Italian yields minus the minimum between the ECB deposit rate and zero. The vertical lines denote August 2014 and February 2016. To improve visibility, the vertical axis is truncated at 4.

Table 1
Cumulative variance explained by principal components.

	OIS	Germany	Italy	Joint
PC1	0.973	0.966	0.930	0.867
PC2	0.999	0.998	0.997	0.970
PC3	1.000	1.000	0.999	0.995
PC4	1.000	1.000	1.000	0.997
PC5	1.000	1.000	1.000	0.999
PC6	1.000	1.000	1.000	0.999

Note: this table reports the cumulative percentage of variance of OIS yields (first column), German yields (second column), Italian yields (third column) and all yields (fourth column) explained by the first six PCs extracted from OIS yields (first column), German yields (second column), Italian yields (third column), and jointly from OIS, German and Italian yields (fourth column).

rate and, from February 2016, German rates diverge even further from the ECB deposit rate. Accordingly, we specify c_t to take the following values:

$$c_t = \begin{cases} 0, & t \leq \text{August 2014} \\ -0.2, & \text{August 2014} < t \leq \text{February 2016} \\ -1, & t > \text{February 2016.} \end{cases} \tag{22}$$

This specification for the lower bound implies that, in the first part of the sample, short-term interest rates are bounded by zero due to the option to convert to currency.[6] In the second part of the sample, short-term interest rates are close to the deposit rate, but, in the last subsample, the effective lower bound differs from the floor for interest rates given by the deposit rate.[7]

5.2. Model specification

The joint shadow rate term structure model in Section 3 allows the risk-free and the country yield curves to be driven by common and country-specific factors. To determine the number of each type of factor, we perform a principal component analysis. We start by analyzing each yield curve separately. The first three columns of Table 1 report the cumulative variance of OIS, German, and Italian zero-coupon yields explained by the corresponding first six principal components (PCs) extracted separately for each country. The table indicates that, for the OIS and the German term structures, the first two PCs explain most of the observed variance (99.9% for OIS and 99.8% for Germany), while for Italy the first three PCs explain 99.9% of the observed variance.

We then pool the three yield curves and extract PCs jointly. The cumulative joint variance of OIS, German, and Italian yields explained by these joint PCs is reported in the last column of Table 1. The table shows that five joint PCs are required

[6] The specification of the lower bound in this part of the sample is in line with Lemke and Vladu (2017).

[7] Preliminary results, available upon request, estimating c_t along with the other coefficients of the model are similar to the ones presented in the paper. However, the lower bound parameter in the last subsample is not stable and depends on the sample used. For this reason, our preferred specification is to calibrate the lower bound parameters.

Table 2
Common factors.

	Germany			Italy		
# OIS PC	PC1	PC2	PC3	PC1	PC2	PC3
1	0.994	0.001	0.000	0.620	0.172	0.011
First 2	0.995	0.965	0.000	0.664	0.739	0.012
First 3	0.995	0.966	0.756	0.743	0.769	0.329
First 4	0.996	0.967	0.833	0.746	0.791	0.356
First 5	0.996	0.967	0.834	0.777	0.794	0.408
First 6	0.996	0.968	0.835	0.777	0.794	0.414

Note: this table reports the R^2 from regressing German and Italian PCs on OIS PCs. The first row refers to regressions on the first OIS PC, the second row refers to regressions on the first two OIS PCs, and so on.

Table 3
Country factors.

	Germany			Italy		
	Yields	1 OIS PC	2 OIS PC	Yields	1 OIS PC	2 OIS PC
1 Country PC	0.966	0.664	0.633	0.930	0.878	0.951
2 Country PC	0.032	0.232	0.203	0.067	0.114	0.040
3 Country PC	0.002	0.095	0.134	0.002	0.006	0.006
4 Country PC	0.000	0.007	0.024	0.001	0.002	0.002
5 Country PC	0.000	0.002	0.004	0.000	0.000	0.000
6 Country PC	0.000	0.001	0.001	0.000	0.000	0.000

Note: this table reports the percentage of variance of German (first three columns) and Italian (last three columns) yield residuals explained by the first 6 country PCs. The first and the fourth column refer to the percentage of variance of German and Italian yields. The second and fifth column refer to the percentage of variance of the residuals of German and Italian yields after they are regressed on the first OIS factor. The third and the sixth refer to the percentage of variance of the residuals of German and Italian yields after they are regressed on the first two OIS factors.

to explain at least 99.9% of the joint variation in OIS, German and Italian yields. This indicates that the German and Italian yield curves are driven by country-specific factors, in addition to common factors.

Given that the OIS yield curve is driven only by the risk-free factors, the PCs extracted from the OIS yield curve proxy for the common risk-free factors. To assess the relation of the common risk-free factors to the country factors, we analyze how much of the variation in the first three country PCs is explained by the OIS factors. In Table 2, we report the R^2 from regressing German and Italian PCs on the OIS PCs. The table indicates that the first German PC is perfectly explained by the first OIS PC, and that the second German PC is mostly explained by the second OIS PC. The PCs extracted from Italian yields are less related to the OIS PCs, and even using all six OIS PCs we can only explain up to 78%, 79% and 41% of the first three Italian PCs, indicating that Italian yields are driven by a strong country-specific component.

To assess the number of country-specific factors, we extract country PCs from the residuals of the regression of German and Italian yields on the first one or two OIS PCs. In Table 3, we report the percentage of variance of German and Italian residuals explained by the first six country PCs. For comparison, in the first and the fourth column we report the explained variance of German and Italian yields when no common components are extracted (this replicates the information reported in Table 1). The table indicates that, after taking into account the two common factors, Italian yields are driven by two country factors, as the first PC extracted from the residuals explains a large proportion of the variance, and the second PC still has an explanatory power that is an order of magnitude larger than the third one. For German yields, the evidence for country-specific factors is less clear.

Overall, Tables 1–3 suggest that five factors are needed to explain the three yield curves; two of these factors are the common OIS factors, one is specific to Germany, and two are specific to Italy. Accordingly, in specifying our model we choose $n = 5,\ n_0 = 2,\ n_{GE} = 1$ and $n_{IT} = 2$.

6. Inference

6.1. Estimation

We estimate the joint shadow rate term structure model by quasi maximum likelihood using a state space representation. The sample consists of panels for $y^0_{t,\tau}$, $y^{GE}_{t,\tau}$ and $y^{IT}_{t,\tau}$, $t = 1, \dots, T$ and $\tau = \tau_1, \dots, \tau_K$. Let us denote the observed yields by:

$$\mathbf{y}_t = (\mathbf{y}_t^{0\prime}, \mathbf{y}_t^{GE\prime}, \mathbf{y}_t^{IT\prime})',$$

with $\mathbf{y}_t^0 = (y_{t,\tau_1}^0, \ldots, y_{t,\tau_K}^0)'$, $\mathbf{y}_t^{GE} = (y_{t,\tau_1}^{GE}, \ldots, y_{t,\tau_K}^{GE})'$ and $\mathbf{y}_t^{IT} = (y_{t,\tau_1}^{IT}, \ldots, y_{t,\tau_K}^{IT})'$, and the model implied yields by:

$$\mathbf{h}(\mathbf{x}_t) = [\mathbf{h}^0(\mathbf{x}_t)', \mathbf{h}^{GE}(\mathbf{x}_t)', \mathbf{h}^{IT}(\mathbf{x}_t)']',$$

with $\mathbf{h}^0(\mathbf{x}_t) = [h_1^0(\mathbf{x}_t), \ldots, h_K^0(\mathbf{x}_t)]'$, $\mathbf{h}^{GE}(\mathbf{x}_t) = [h_1^{GE}(\mathbf{x}_t), \ldots, h_K^{GE}(\mathbf{x}_t)]'$ and $\mathbf{h}^{IT}(\mathbf{x}_t) = [h_1^{IT}(\mathbf{x}_t), \ldots, h_K^{IT}(\mathbf{x}_t)]'$. The elements of $\mathbf{h}(\mathbf{x}_t)$ were defined in (10). We write the measurement equation as:

$$\mathbf{y}_t = \mathbf{h}(\mathbf{x}_t) + \mathbf{u}_t, \tag{23}$$

where the measurement error $\mathbf{u}_t$ is IID normally distributed with mean zero. We assume that measurement errors are uncorrelated (across countries and maturities) and with a variance that depends on the country but not on the yield maturity. The three measurement error standard deviations ω^0, ω^{GE} and ω^{IT} must be estimated with the other parameters.

The transition equation is given by

$$\mathbf{x}_{t+1} = \mu + \mathbf{\Phi}\mathbf{x}_t + \mathbf{v}_t \tag{24}$$

where $\mathbf{v}_t \sim \mathcal{N}_{IID}(\mathbf{0}, \mathbf{\Sigma})$, and $\mathbf{\Sigma} = \mathbf{\Gamma}\mathbf{\Gamma}'$.

The measurement equation in (23) is nonlinear in the state variables. Therefore, we base quasi maximum likelihood inference on the Extended Kalman filter. Appendices Appendix A and Appendix B provide additional details on the estimation procedure.

6.2. Identification

To uniquely identify the latent states, we use an identification scheme similar to Dai and Singleton (2000) and impose $\mathbf{\Gamma} = \mathbf{I}_n$, $\delta_1^0 \geq 0$, $\delta_1^{GE} \geq 0$, $\delta_1^{IT} \geq 0$, $\mu = \mathbf{0}$ and $\mathbf{\Phi}^{\mathbb{Q}}$ lower triangular. This implies that the full parameter vector $\boldsymbol{\theta}$ is given by:

- δ_0^0, δ_0^{GE}, δ_0^{IT} (3 parameters),
- δ_1^0, δ_1^{GE}, δ_1^{IT} ($n + 2n_0$ parameters),
- $\mathbf{\Phi}^{\mathbb{Q}}$ ($\frac{n(n+1)}{2} - n_{GE}n_{IT}$ parameters),
- $\mu^{\mathbb{Q}}$ (n parameters),
- $\mathbf{\Phi}$ (n^2 parameters),
- $\omega^0, \omega^{GE}, \omega^{IT}$ (3 parameters)

Preliminary estimates indicate that the first elements of δ_1^{GE} and δ_1^{IT} are equal to zero, so fixing $\left(\delta_1^{GE}\right)_1 = 0$ and $\left(\delta_1^{IT}\right)_1 = 0$ we have a total of $4 + 2n_0 - n_{GE}n_{IT} + \frac{5n+3n^2}{2}$ parameters. For the specification selected in Section 5.2, we have $n = 5$, $n_0 = 2$, $n_{GE} = 1$ and $n_{IT} = 2$, implying a total of 56 parameters to be estimated.

We impose stationarity under $\mathbb{Q}$ by constraining the diagonal elements of $\mathbf{\Phi}^{\mathbb{Q}}$ between 0 and 1; we also enforce stationarity under $\mathbb{P}$ by imposing that all the eigenvalues of $\mathbf{\Phi}$ are strictly smaller than 1.

7. Results

In the next three sections we present the model estimation results, the estimated shadow rates and shadow spreads, and the implications of the interest rate lower bound for the properties of sovereign spreads.

7.1. Estimation results

Table 4 reports quasi maximum likelihood estimates of the parameters of our joint shadow rate model for OIS, German, and Italian term structures based on yields observed between January 2001 and January 2020. According to these estimates, the latent factors are less persistent under the actual probability measure $\mathbb{P}$ than under the risk-neutral measure $\mathbb{Q}$. The estimate of the shadow short rate parameters δ_1^0 suggests that the second common factor drives the OIS and the German shadow short rates, while the two Italian factors both drive the Italian shadow short rate. In addition, we can see that the Italian factors have a stronger effect on the Italian shadow short rate than the German factor on the corresponding shadow short rate.

The average yield curve fit, reported in Fig. 5, is good for the three yield curves both in the full sample (from 2001 to 2020), in the pre-lower bound subsample (from 2001 to 2011) and in the lower bound subsample (from 2012 to 2020). The root mean square errors (RMSE) in Table 5 indicate that, in the second subsample, the model fits slightly better OIS and German yields than for Italian yields. The table also indicates that the performance of the model is slightly better in the lower bound period, with an average RMSE of 0.061, compared with a RMSE of 0.084 in the pre-lower bound period. In the first subsample, the six month maturity has the largest RMSE for the German and the OIS rates, while for Italian yields in both subsamples the largest RMSE is for the 10-year rate.

In Section 3.3, we decomposed observed yields into shadow yields and lower bound wedges, where the former are linear in the factors and the latter depend on the distance of the shadow forward rates from the lower bound and the volatilities of shadow rates under $\mathbb{Q}$. To assess the magnitude of the lower bound wedge, we estimated $\sigma_\tau^i -$ the volatility under $\mathbb{Q}$ of the shadow rate with maturity $\tau -$ as in Eq. (8) for the three term structures. Fig. 6 plots the estimates with respect to the

Table 4
Estimated parameters.

$\mu^{\mathbb{Q}}$	$\mathbf{\Phi}^{\mathbb{Q}}$				
0.079***	0.992***	0	0	0	0
(0.017)	(0.001)				
0.042	0.033***	0.986***	0	0	0
(0.066)	(0.003)	(0.002)			
0.000	0.030***	-0.013	0.997***	0	0
(0.068)	(0.008)	(0.005)	(0.005)		
0.087***	0.007	-0.005	0	0.992***	0
(0.018)	(0.006)	(0.001)		(0.002)	
0.001	0.008	0.013	0	0.059**	0.920***
(0.224)	(0.013)	(0.015)		(0.025)	(0.019)

$\mathbf{\Phi}$					δ_1^0	δ_1^{GE}	δ_1^{IT}
0.991***	0.024	-0.062	-0.023	-0.002	0.008*	0	0
(0.021)	(0.019)	(0.045)	(0.043)	(0.063)	(0.004)		
0.009	0.957***	0.045	-0.038	0.004	0.206***	0.211***	0.077
(0.038)	(0.053)	(0.091)	(0.100)	(0.133)	(0.021)	(0.021)	(0.085)
0.050	-0.032	0.894***	-0.061	0.090	0	0.040***	0
(0.037)	(0.053)	(0.080)	(0.068)	(0.105)		(0.012)	
0.036	0.023	-0.071	0.908***	-0.033	0	0	0.188***
(0.037)	(0.026)	(0.076)	(0.063)	(0.091)			(0.058)
0.000	0.074**	0.036	-0.033	0.728***	0	0	0.294***
(0.033)	(0.037)	(0.053)	(0.086)	(0.150)			(0.057)

Curve	δ_0	ω
OIS	0.949***	0.081***
	(0.213)	(0.004)
GE	0.776***	0.082***
	(0.199)	(0.005)
IT	1.021**	0.096***
	(0.444)	(0.004)

Note: this table reports the estimated parameters of the joint shadow rate term structure model for OIS, German, and Italian yields. Asymptotic standard errors computed using the QML sandwich formula are reported in brackets. *, **, and *** denote significance at the 10%, 5%, and 1% level.

maturity τ. It is apparent that the estimated volatility for German and OIS future shadow rates is similar at all maturities, while the estimated Italian volatility is larger for all τ. This implies that for the same distance between shadow forward rates and the lower bound, Italian yields contain a larger lower bound wedge, see (13), (17) and Fig. 1.

7.2. Observed rates and shadow rates

To illustrate the effect of the lower bound on observed yields, Fig. 7 reports OIS, German and Italian observed yield curves on two dates. The first date is April 2013, when OIS and German short rates were at the lower bound, but Italian rates remained far above it. The second date is February 2015, when short-term OIS and German yields were negative, and the 6-month Italian yield was close to the lower bound.

In the figure, we report observed yields, fitted yields, and shadow yields, defined in (15). In April 2013, observed, fitted, and shadow Italian yields coincided. Instead, shadow OIS and German yields were below the observed yields and negative for short maturities. In February 2015, shadow Italian yields were also below the observed yields, and negative for short rates. However, OIS and German shadow yields were negative for all maturities, indicating that, at this date, OIS and German lower bound wedges were large at any maturity. In addition, in both dates, the short ends of the OIS and the German yield curves are flat, which is a feature of the yield curve at the lower bound that can be fitted well by a shadow rate model (see Wu and Xia, 2020).

In Fig. 8, we report the time series of the 10-year yields and shadow yields. The figure shows that, since mid-2011, the OIS and German 10-year shadow yields are lower than the observed yields. The Italian 10-year shadow yield becomes lower than the observed yield only in 2014. The time series plot of the lower bound wedges shows that OIS and German 10-year yields have been constrained by the lower bound since mid-2011 and that the effect of the constraint has been stronger on the German 10-year rate than on the OIS rate. The figure also shows that the Italian lower bound wedge was non-zero before the interest rates reached the lower bound. This can be explained by the large estimated Italian volatilities of shadow rates under $\mathbb{Q}$, as shown in Fig. 6. The Italian lower bound wedge increases in 2014 and reaches the same level as the OIS lower bound wedge in 2015.

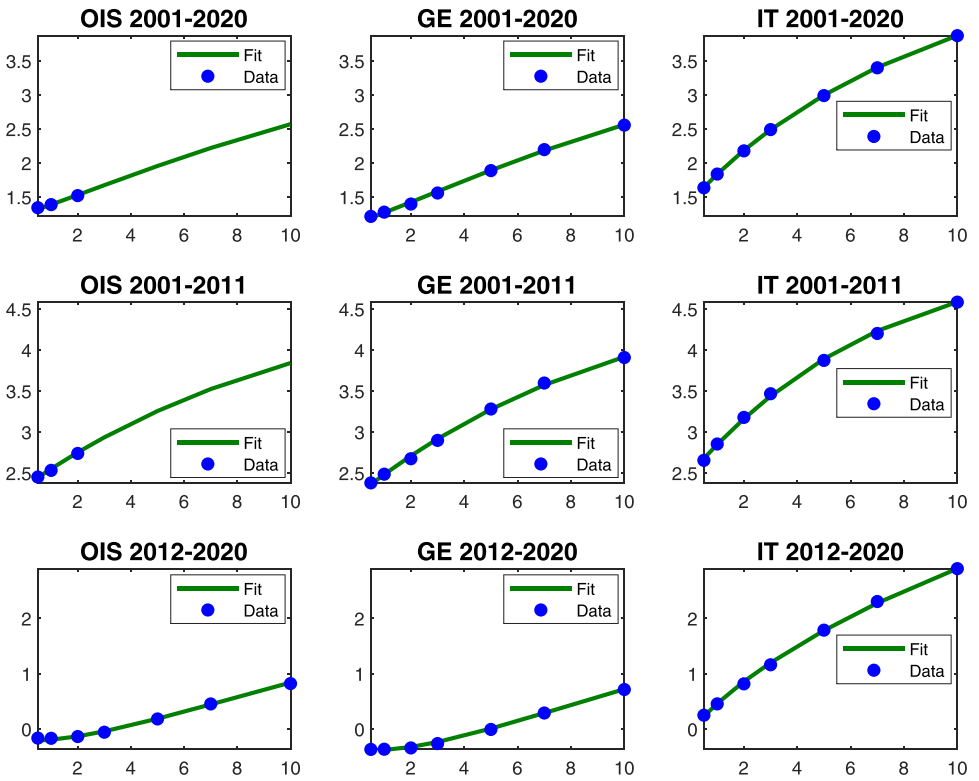

Fig. 5. Fitted yield curves. This figure reports average OIS, German, and Italian yield curves on the full sample (top plot), the pre-lower bound subsample (middle plot), and the lower bound subsample (bottom plot). The lines refer to the model fit of the joint shadow rate term structure model and the dots refer to the observed data.

Table 5
RMSE

Full sample 2001-2020								
	0.5	1	2	3	5	7	10	Average
OIS	0.113	0.066	0.075	0.067	0.054	0.041	0.062	0.068
GE	0.114	0.045	0.083	0.083	0.061	0.044	0.086	0.074
IT	0.093	0.059	0.101	0.091	0.058	0.066	0.118	0.084
Average	0.107	0.057	0.086	0.081	0.058	0.050	0.089	0.075
Subsample 2001-2011								
	0.5	1	2	3	5	7	10	Average
OIS	0.127	0.067	0.093	0.086	0.062	0.048	0.078	0.080
GE	0.142	0.046	0.100	0.095	0.063	0.050	0.093	0.084
IT	0.104	0.067	0.112	0.095	0.053	0.072	0.115	0.088
Average	0.124	0.060	0.101	0.092	0.060	0.056	0.095	0.084
Subsample 2011-2020								
	0.5	1	2	3	5	7	10	Average
OIS	0.091	0.064	0.040	0.046	0.046	0.034	0.046	0.052
GE	0.058	0.043	0.051	0.064	0.057	0.034	0.076	0.055
IT	0.076	0.046	0.085	0.085	0.064	0.059	0.121	0.077
Average	0.075	0.051	0.059	0.065	0.056	0.042	0.081	0.061

Note: this table reports the root mean square error of the joint shadow rate term structure model for OIS, German, and Italian yields on the full sample (top panel), the pre-lower bound subsample (middle panel), and the lower bound subsample (bottom panel).

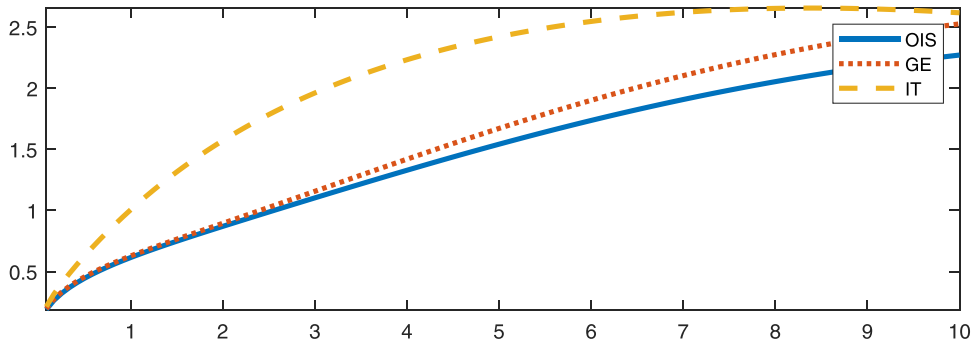

Fig. 6. Forward rate volatility under the risk-neutral measure. This figure reports the estimated forward rate volatility under the risk-neutral measure in Eq. (8) obtained from the joint shadow rate term structure model for OIS, German, and Italian yields.

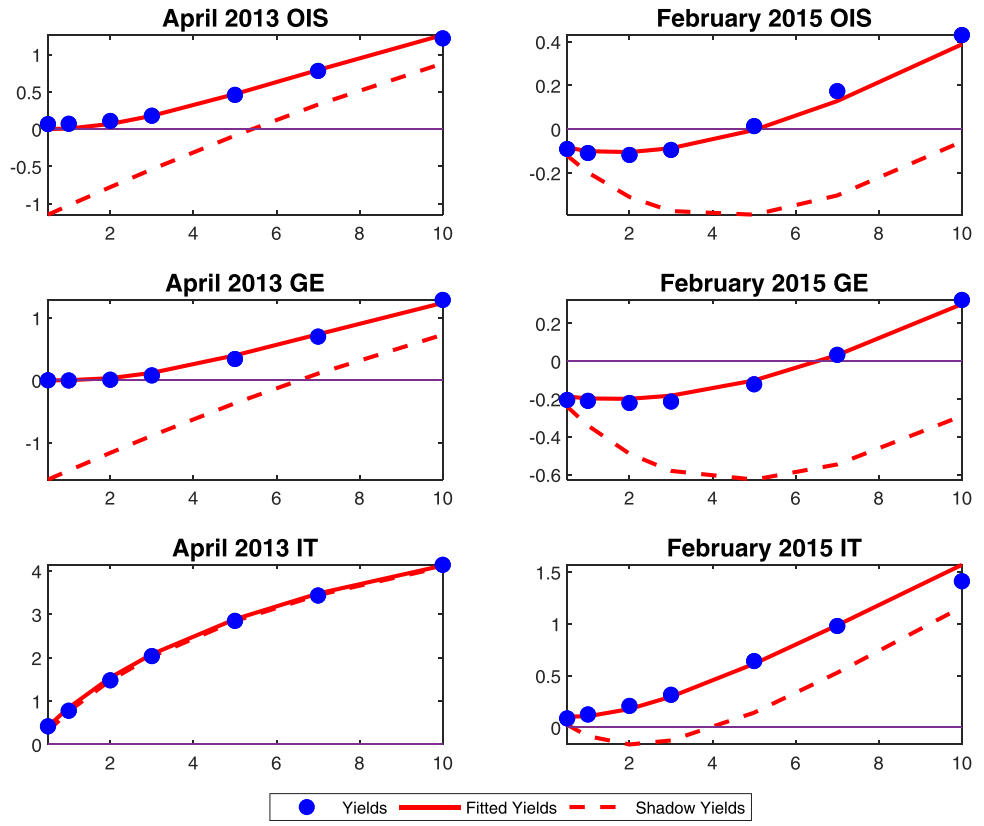

Fig. 7. Yield curves on two selected dates. This figure reports OIS, German, and Italian yield curves on two selected dates: April 2013 (left plots) and February 2015 (right plots). The blue denote the observed yields, the continuous line denotes the fitted yields defined in (10) and the dashed line denotes the shadow yields defined in (15).

Sovereign spreads, shadow spreads and spread wegdes are reported in Fig. 9. The figure indicates that the joint shadow rate term structure model for OIS, German, and Italian yields fits well all 10-year spreads. We can also see that the 10-year German-OIS spread is smaller than the Italian-OIS and the Italian-German spreads in the sample period. As for the difference between observed spreads and shadow spreads, the figure shows that the German-OIS shadow spread is lower than the observed spread since mid-2011; on the contrary, during the same period the Italian-OIS and the Italian-German shadow spreads are larger than the corresponding observed spreads.

The time series of the sovereign spread wedges—i.e. the nonlinear components of spreads—show that, when interest rates reached the lower bound, the German-OIS spread wedge became large and positive, while the Italian-OIS and the Italian-

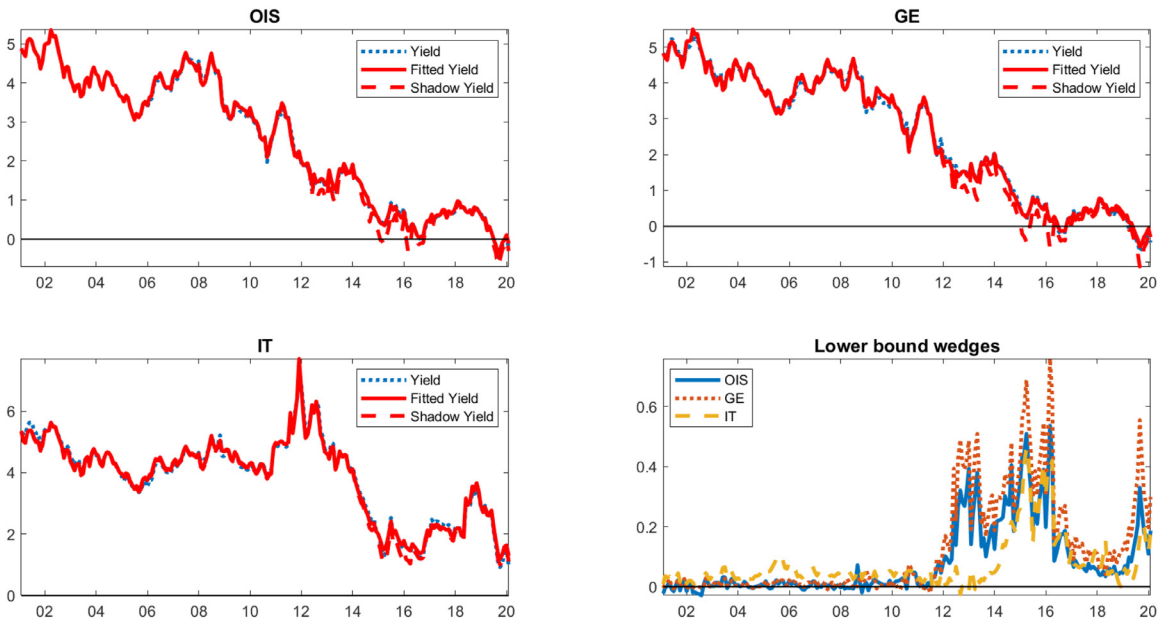

Fig. 8. 10-year yields, shadow yields and lower bound wedges. This figure reports 10-year yields, shadow yields, and lower bound wedges for OIS, Germany, and Italy. In the top plots and the bottom left plot, the dotted line denotes observed yields, the continuous line denotes fitted yields as in (10) and the dashed line denotes the shadow yields as in (15). The bottom right plot reports the lower bound wedges for the 10-year OIS, German, and Italian yields, computed as in (17).

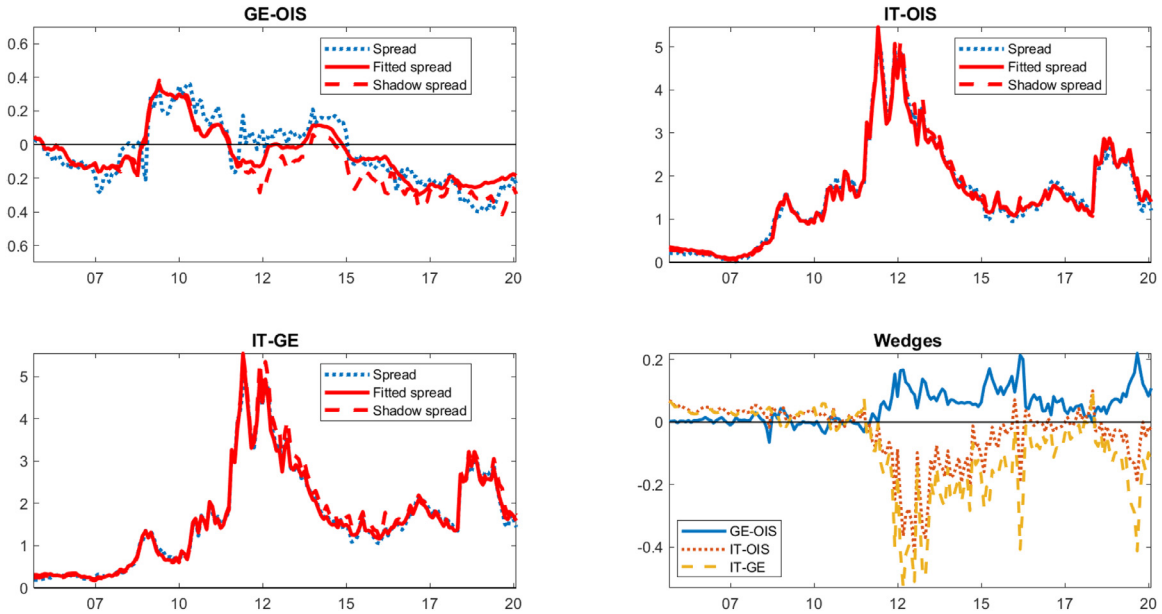

Fig. 9. 10-year spreads, shadow spreads, and spread wedges. This figure reports 10-year spreads, shadow spreads, and spread wedges for OIS, Germany, and Italy. In the top plots and the bottom left plot, the dotted line denotes observed spreads, the continuous line denotes fitted spreads and the dashed line denotes the shadow spreads. The bottom right plot reports the lower bound spread wedges for the 10-year GE-OIS, IT-OIS and IT-GE spreads. Shadow spreads and lower bound spread wedges are computed as in (19).

German spread wedges became large and negative. This is in line with our discussion in Section 4 regarding the sign of the sovereign spread wedge and the presence of sovereign risk or convenience yield. The German-OIS sovereign spread wedge is positive because, due to the safety premium on German bonds, German short rates are closer to the lower bound, and thus more constrained than OIS rates. On the contrary, due to the presence of sovereign risk, Italian short rates are larger than OIS and German rates, which implies that they are less constrained by the lower bound. As a consequence, Italian-OIS and Italian-German spread wedges are negative. Summary statistics for the sovereign spread wedges, reported in Table 6,

Table 6
Summary statistics of Sovereign Spread Wedges .

	Mean	Std	Min	Max	Q(25)	Q(75)
GE-OIS	0.048	0.054	-0.065	0.221	0.005	0.082
IT-OIS	-0.036	0.096	-0.423	0.100	-0.072	0.030
IT-GE	-0.084	0.137	-0.532	0.100	-0.154	0.028

Note: this table reports summary statistics for the 10-year sovereign spread wedges of Germany with respect to the OIS, Italy with respect to OIS, and Italy with respect to Germany.

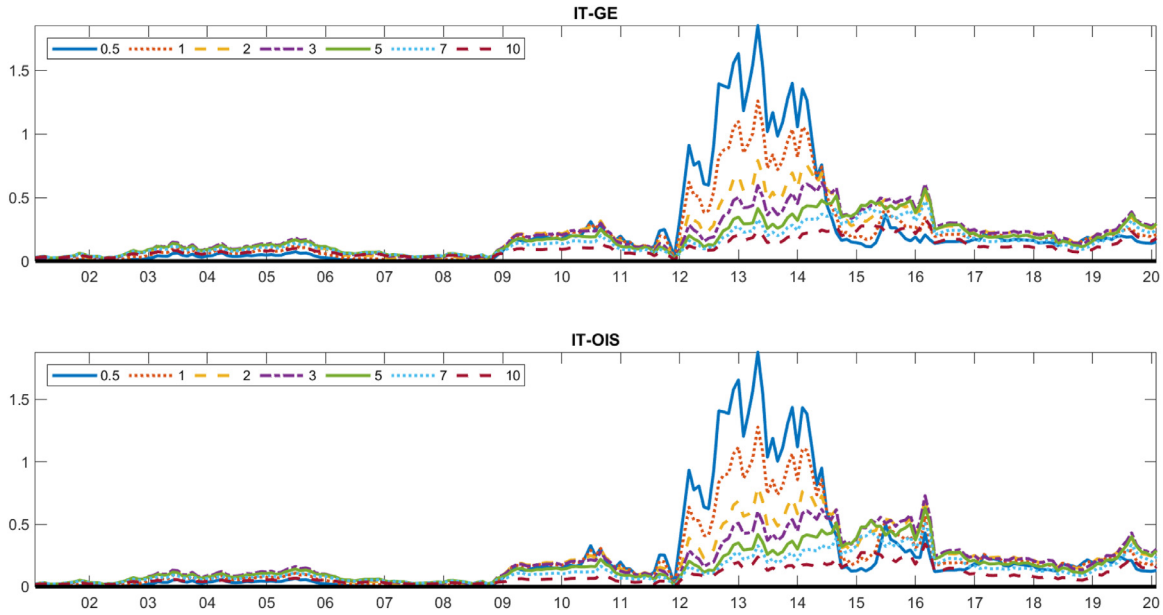

Fig. 10. Skewness of Spread Distributions. This figure reports the skewness index of the $\mathbb{P}$-distribution of 12-month ahead sovereign spreads of Italy with respect to Germany (top panel) and with respect to OIS (bottom panel) at the 7 observed maturities. In each point in time, we use the estimated parameters and factors to simulate 20,000 paths of factors 12-months ahead using (2). Then substituting in (10), we obtain 20,000 simulated yields 12-months ahead, from which we compute the asymmetry index.

show that in our sample they reached a maximum of 0.22% for German-OIS spreads and a minimum of -0.42% and -0.53% for, respectively, Italian-OIS and Italian-German spreads. As for the timing of the peaks in sovereign spread wedges, notice that, as shown in Eq. (20), the sovereign spread wedge is given by the difference in the lower bound wedges of the two long-term rates, i.e. by the differential impact of the lower bound on the two long-term rates. Given that in 2012 German and OIS rates reach the lower bound but Italian rates remain far from it, this is the period when the Italian sovereign spread wedges are the largest.

7.3. Effects of the lower bound on sovereign spreads

The fact that sovereign spread wedges become non-negligible when term structures are close to the lower bound has three important implications for the properties of long-term sovereign bond spreads at the interest rate lower bound.

First, the distribution of observed spreads becomes skewed as interest rates approach the lower bound. To assess this feature, for each date in the sample we simulated 20,000 trajectories of the latent factors over a 12-month horizon under the physical measure $\mathbb{P}$, starting from their updated estimates obtained from the Extended Kalman filter. Fig. 10 plots the skewness of the distribution of the 12-month ahead simulated spreads for Italian yields with respect to Germany and OIS against the date at which the trajectories were started. If we compare this with Fig. 3, it is clear that the skewness is very sensitive to the distance of the short end of the term structure from the lower bound. Before 2009, when all interest rates were sufficiently far from the lower bound, the distribution of the simulated spreads was fairly symmetric, but things changed significantly after 2009, when rates approached the lower bound. Note that the 5% critical threshold for a two-sided z-test of the null of zero skewness is 0.034; hence, the null of a symmetric distribution is rejected for all dates after 2009.

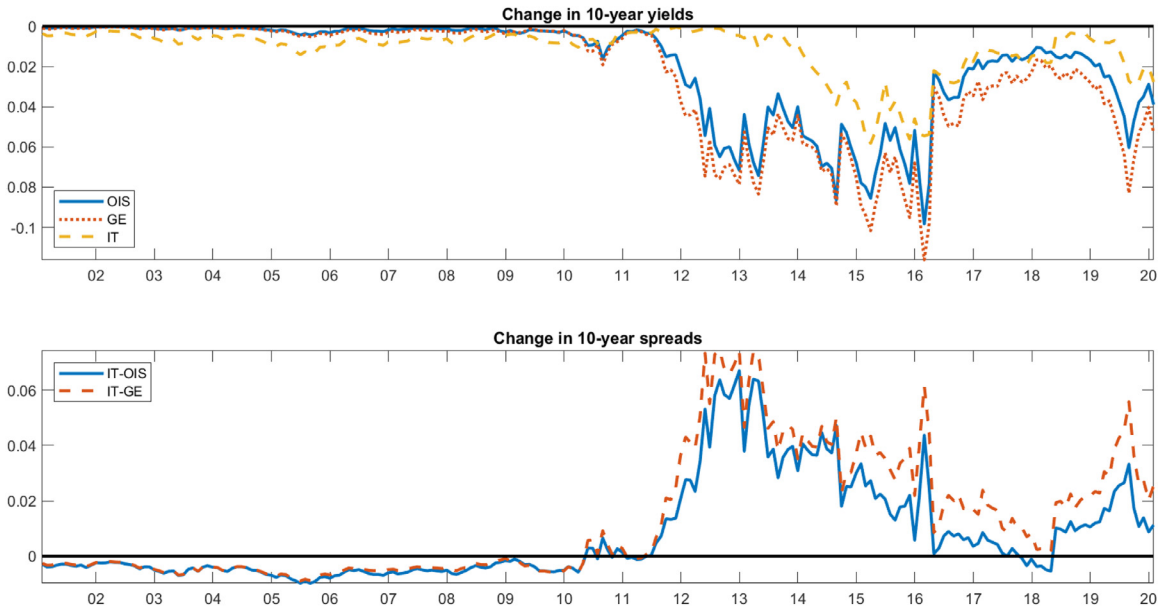

Fig. 11. Effect of a lower bound shift of -0.20%. This figure reports the effects of a shift of the lower bound of -0.20% on the 10-year OIS, German, and Italian yields (top plot), and on the 10-year IT-OIS and IT-GE sovereign spreads (bottom plot). In the top plot, at each point in time, we report the difference between the counterfactual 10-year yields (computed by lowering the lower bound in (10) by 0.20%) and the fitted yields. In the bottom plot, at each point in time, we report the difference between the counterfactual 10-year sovereign spread (computed from the counterfactual 10-year yields) and the fitted spread.

It is also apparent that the skewness is more pronounced the shorter the maturity of the spread under consideration, but is nonetheless also significant for the 10-year spread.

A second implication of the interest rate lower bound on sovereign spreads is that, because observed spreads depend on the distance from the lower bound, an exogenous change in the latter affects observed spreads, even if the sovereign risk does not change. Fig. 11 illustrates this feature for the case of the Italian-OIS and Italian-German 10-year spreads. In the top plot, for each date in the sample, we report the difference between the counterfactual 10-year yields, obtained after a 20 basis points reduction in the lower bound, and the fitted yields. The effect of a shift in the lower bound on the 10-year yields clearly changes after the short rates of each country reach the lower bound: 2011 for the German and OIS rates, and 2015 for the Italian rate. Up to 2010, the decrease in the lower bound would not have any effect on the 10-year OIS and German yields, after this date the effect would be a decrease of the 10-year OIS and German rates by as much as 10 or 12 basis points, respectively. As for the Italian 10-year yield, the decrease in the lower bound would always have a negative effect on the yield. This is due to the large risk-neutral volatility of the shadow forward rates, reported in Fig. 7, which increases the option value of cash. However, the effect of the decrease in the lower bound on the Italian 10-year yield also becomes larger when short-term Italian rates reach the lower bound.

In the bottom plot of Fig. 11, at each point in time, we report the difference between the counterfactual 10-year Italian sovereign spreads, obtained after the 20 basis points reduction in the lower bound, and the fitted 10-year Italian spreads. The effect of the decrease in the lower bound on long-term Italian spreads changes around mid-2011. Up to that date, the decrease in the lower bound would decrease all spreads by less than a basis point. After this date the effect changes sign and becomes much larger, as the same decrease in the lower bound would increase 10-year Italian spreads by as much as 7 basis points. Notice that, as shown in (21), the lower bound depends on the deposit rate of the Eurosystem, which is a monetary policy instrument under the control of the European Central Bank. Therefore, results in Fig. 11 indicate that when short-term rates are constrained by the lower bound, a monetary policy easing increases sovereign spreads, even if it does not affect the sovereign risk. In reality, a reduction in the ECB deposit rate can also potentially affect all the state variables, implying that any assessment of the effect of such a policy on sovereign spreads needs to take into account the nonlinearities that are caused by the differential impact of the lower bound on the two long-term interest rates. As shown in Fig. 11, this is going to be particularly important when one yield curve reaches the lower bound and the other one is far from it, as occurs in our data for Germany and Italy in 2012; it is also relevant when one yield curve has moved away from the lower bound and the other is still close to it, as will happen when euro area risk-free rates start to increase.

A third and final implication of the existence of an interest rate lower bound on the properties of long-term bond spreads is that, when the constraint is binding, the observed spread loses its informative content about the sovereign risk, but the shadow spread does not. To check this, we regress the 10-year observed and shadow bond spreads between Germany and

Table 7
Sovereign government bonds and credit default swaps.

Dependent var.	$\Delta_{t,10}^{IT,GE}$	$\tilde{\Delta}_{t,10}^{IT,GE}$	$\Delta_{t,10}^{IT,GE}$	$\tilde{\Delta}_{t,10}^{IT,GE}$
Constant	-0.01	-0.02	-0.04	-0.05
	(0.04)	(0.05)	(0.05)	(0.05)
$CDS_t^{IT,GE}\mathbb{I}_{t<1/2012}$	0.53***	0.62***	0.45***	0.50***
	(0.10)	(0.11)	(0.09)	(0.09)
$CDS_t^{IT,GE}\mathbb{I}_{t\geq 1/2012}$	0.42***	0.55***	0.33***	0.44***
	(0.09)	(0.11)	(0.07)	(0.09)
$\Delta_{t-1,10}^{IT,GE}$	0.71***		0.79***	
	(0.06)		(0.05)	
$\tilde{\Delta}_{t-1,10}^{IT,GE}$		0.65***		0.75***
		(0.07)		(0.05)
R^2	0.94	0.94	0.91	0.91
Wald	8.46***	2.25	5.41**	1.62
N	145	145	134	134
Excluded observations	-	-	Oct 2011 - Aug 2012	Oct 2011 - Aug 2012

Note: this table reports regression parameters of 10-year IT-GE bond spreads and shadow bond spreads on 10-year CDS spreads between Italy and Germany. HAC standard errors with 5 lags and Bartlett kernel are reported in brackets. *, ** and *** denote significance at the 10%, 5% and 1% level. The Wald test statistic refers to the test of equality of the coefficients on CDS spreads. Results in the first two columns are based on the full sample and results in the last two columns exclude observations from October 2011 to August 2012.

Italy on the 10-year CDS spread between the two countries.[8] Each regression allows for one lag of the dependent variable and also enables the CDS spread parameter to take different values in the periods before and after January 2012. Table 7 illustrates the estimation results and also reports the Wald test statistic of the null of equal CDS spread slope in the two subperiods. All tests are computed using the robust HAC variance matrix. Results in the first two columns are based on the full sample, while results in the last two columns exclude observations from October 2011 to August 2012 (the period in which the Italian bond market was subject to large volatility). The full sample results show that the yield spread coefficient on CDS spreads decreases from 0.53 before January 2012 to 0.42 after the same date; the robust Wald test of equal slopes rejects the null at the 1% level. The shadow yield spread estimates provide a different conclusion: the two slope parameters are more similar and the robust Wald test fails to reject the null of equal slopes. Results excluding observations from October 2011 to August 2012 are similar. We therefore conclude that the relation between the CDS spread and the shadow yield spread was not affected by the lower bound on interest rates. On the contrary, the relation between CDS spreads and the observed yield spread changed significantly after 2012, when German short-term rates reached the lower bound.

8. Conclusion

This paper studies the effect of the interest rate lower bound on spreads between long-term sovereign yields in the euro area. We develop a joint shadow rate term structure model for three yield curves: the risk-free yield curve proxied by OIS rates, the German yield curve, and the Italian yield curve. This framework allows us to model the nonlinear relation between sovereign spreads and sovereign risk when interest rates are close to the lower bound.

Our results highlight the presence of strong nonlinearities in the behavior of long-term sovereign spreads at the interest rate lower bound, and call for the development of structural models for sovereign spreads that take into account the existence of a lower bound.

While our analysis focuses on the sovereign spread of Italian long-term bonds with respect to euro area risk-free and German bonds, the setup can be readily applied to any other euro area country. Further work in this area will involve the development of multi-country multi-currency shadow rate models that allow to investigate the joint behavior of interest rates and exchange rates at the lower bound. Another interesting avenue for further research is allowing investors to price time variations in the lower bound in shadow rates models with multiple yield curves, along the lines of Wu and Xia (2020).

Appendix A. Estimation of the shadow rate term structure model

The state space representation of the shadow rate term structure model is

$$\begin{aligned} \mathbf{y}_t &= \mathbf{h}(\mathbf{x}_t) + \mathbf{u}_t, & \mathbf{u}_t &\sim \mathcal{N}_{IID}(\mathbf{0}, \boldsymbol{\Omega}) \\ \mathbf{x}_{t+1} &= \boldsymbol{\mu} + \boldsymbol{\Phi}\mathbf{x}_t + \mathbf{v}_t, & \mathbf{v}_t &\sim \mathcal{N}_{IID}(\mathbf{0}, \boldsymbol{\Sigma}). \end{aligned}$$

[8] The theoretical equivalence of CDS prices and credit spreads has been derived by Duffie (1999) and verified empirically by Blanco et al. (2005). However, since the 2008 financial crisis, several studies document the emergence of a CDS-bond basis, i.e. a difference between the premium on the CDS and the credit spread on the underlying bond. In particular, the basis between euro area sovereign CDS and government bonds is investigated in Fontana and Scheicher (2016).

where $\mathbf{\Sigma} = \mathbf{\Gamma}\mathbf{\Gamma}'$ and $\mathbf{\Omega}$ is diagonal with variances equal to $(\omega^0)^2$, $(\omega^{GE})^2$ and $(\omega^{IT})^2$ for measurement errors on OIS, German and Italian yields, respectively.

- We use a diffuse initialization of the Extended Kalman filter, as follows

$$\widehat{\mathbf{x}}_{1|0} = \mathrm{E}(\mathbf{x}_1) = (\mathbf{I}_n - \mathbf{\Phi})^{-1}\mu$$

and

$$\mathbf{P}_{1|0} = \mathrm{E}[(\mathbf{x}_1 - \widehat{\mathbf{x}}_1)(\mathbf{x}_1 - \widehat{\mathbf{x}}_1)'] = 100\,\mathbf{I}_n$$

- The forecasts of the observables and their approximate MSEs are given by:

$$\widehat{\mathbf{y}}_{t|t-1} = \mathbf{h}(\widehat{\mathbf{x}}_{t|t-1}), \quad t = 1, \ldots, T$$

and

$$\mathrm{E}[(\mathbf{y}_t - \widehat{\mathbf{y}}_{t|t-1})(\mathbf{y}_t - \widehat{\mathbf{y}}_{t|t-1})'] \approx \widehat{\mathbf{H}}'_{t|t-1}\mathbf{P}_{t|t-1}\widehat{\mathbf{H}}_{t|t-1} + \mathbf{\Omega}, \quad t = 1, \ldots, T,$$

where $\widehat{\mathbf{H}}_{t|t-1} = \mathbf{H}(\widehat{\mathbf{x}}_{t|t-1})$, and

$$\mathbf{H}(\mathbf{x}_t)' = \begin{bmatrix} \mathbf{H}^0(\mathbf{x}_t)' \\ \mathbf{H}^{GE}(\mathbf{x}_t)' \\ \mathbf{H}^{IT}(\mathbf{x}_t)' \end{bmatrix}$$

with

$$\mathbf{H}^i(\mathbf{x}_t)' = \begin{bmatrix} \partial h_1^i(\mathbf{x}_t)/\partial \mathbf{x}_t' \\ \vdots \\ \partial h_K^i(\mathbf{x}_t)/\partial \mathbf{x}_t' \end{bmatrix}, \text{ for } i = 0,\ GE,\ IT.$$

Since $g'(z) = N(z)$, we get

$$\frac{\partial h_\tau^i(\mathbf{x}_t)}{\partial \mathbf{x}_t} = \frac{1}{\tau}\left[\mathbb{I}_{\mathbb{R}_+}(s_t^i - \underline{r}_t)\delta_1^i + \sum_{j=1}^{\tau-1} N\left(\frac{a_j^i + \mathbf{b}_j^{i\prime}\mathbf{x}_t^i - \underline{r}_t}{\sigma_j^i}\right)\mathbf{b}_j^i\right], \ i = 0, GE, IT$$

where $\mathbb{I}_{\mathbb{R}_+}(z) = 1$ if $z > 0$, and 0 otherwise.

- Given their forecasted values, the updated values of the state variables are computed as:

$$\widehat{\mathbf{x}}_{t|t} = \widehat{\mathbf{x}}_{t|t-1} + \mathbf{P}_{t|t-1}\widehat{\mathbf{H}}_{t|t-1}(\widehat{\mathbf{H}}'_{t|t-1}\mathbf{P}_{t|t-1}\widehat{\mathbf{H}}_{t|t-1} + \mathbf{\Omega})^{-1}(\mathbf{y}_t - \widehat{\mathbf{y}}_{t|t-1}), \quad t = 1, \ldots, T$$

and

$$\mathbf{P}_{t|t} = \mathbf{P}_{t|t-1} - \mathbf{P}_{t|t-1}\widehat{\mathbf{H}}_{t|t-1}(\widehat{\mathbf{H}}'_{t|t-1}\mathbf{P}_{t|t-1}\widehat{\mathbf{H}}_{t|t-1} + \mathbf{\Omega})^{-1}\widehat{\mathbf{H}}'_{t|t-1}\mathbf{P}_{t|t-1}, \quad t = 1, \ldots, T$$

- Given their updated values, the forecasted values of the state variables are computed as:

$$\widehat{\mathbf{x}}_{t+1|t} = \mu + \mathbf{\Phi}\widehat{\mathbf{x}}_{t|t}, \quad t = 1, \ldots, T-1$$

and

$$\mathbf{P}_{t+1|t} = \mathbf{\Phi}\mathbf{P}_{t|t}\mathbf{\Phi}' + \mathbf{\Sigma}, \quad t = 1, \ldots, T-1$$

- Finally, the likelihood function is computed using the recursive factorization:

$$\mathbf{y}_t|\mathbf{Y}_{t-1} \sim \mathcal{N}(\widehat{\mathbf{y}}_{t|t-1}, \widehat{\mathbf{H}}'_{t|t-1}\mathbf{P}_{t|t-1}\widehat{\mathbf{H}}_{t|t-1} + \mathbf{\Omega}), \quad t = 2, \ldots, T.$$

Appendix B. Computational details

It is well known that the likelihood surfaces of Gaussian affine term structure models are highly nonlinear and characterized by several local maxima, and it is likely that these features are shared by shadow rate models. Therefore, special attention was devoted to the numerical maximization procedures required by parameter estimation. The loglikelihood function based on the Extended Kalman Filter was maximized using a specifically written Fortran code. We considered 2,400 randomly drawn starting values of the parameters, chosen in accordance with the suggestions Hamilton and Wu (2012). Specifically, we set the same initial guess for $\mathbf{\Phi}$ and $\mathbf{\Phi}^{\mathbb{Q}}$, a $(n \times n)$ diagonal matrix with nonzero entries generated from a $\mathcal{U}(0.5, 1)$ distribution. We parameterized both matrices to impose the stationarity of the state variables process. The remaining parameters were set at reasonable values: each element of δ_1 and ω was initialized at 0.01, while the elements of $\mu^{\mathbb{Q}}$ and the lower bound parameters were initialized at 0.

The numerical optimization of the loglikelihood was conducted in two steps. In the first, the target function was maximized using the derivative free politope algorithm introduced by Nelder and Mead (1965), which is relatively robust in regions of the parameter space that lie away from the maximum. In the second step, we started a derivative-based optimization algorithm at the point of convergence obtained in the first step in order to accelerate convergence to the maximum. We

used the L-BFGS algorithm introduced by Liu and Nocedal (1989), with analytical derivatives computed using the Tapenade AD engine Hascoet and Pascual (2013). The first and second analytical derivatives were also used to compute the asymptotic standard error of the estimates, using White (1982) "sandwich" formula. A single loglikelihood optimization takes roughly 20 minutes on a single core. The task was completed on a 24 core x64 workstation.

References

Alesina, A., De Broeck, M., Prati, A., Tabellini, G., 1992. Default risk on government debt in OECD countries. Econ. Pol. 7 (15), 427–463.
Bauer, M.D., Rudebusch, G.D., 2016. Monetary policy expectations at the zero lower bound. J. Money Credit Bank. 48 (7), 1439–1465.
Beirne, J., Fratzscher, M., 2013. The pricing of sovereign risk and contagion during the European sovereign debt crisis. J. Int. Money Finance 34, 60–82.
Black, F., 1995. Interest rates as options. J. Finance 50 (5), 1371–1376.
Blanco, R., Brennan, S., Marsh, I.W., 2005. An empirical analysis of the dynamic relation between investment-grade bonds and credit default swaps. J. Finance 60 (5), 2255–2281.
Borri, N., Verdelhan, A., 2011. Sovereign risk premia. In AFA 2010 Atlanta Meetings Paper.
Bullard, J., 2012. Shadow interest rates and the stance of US monetary policy. Federal Reserve Bank of St. Louis, 206.
Carriero, A., Mouabbi, S., Vangelista, E., 2018. UK term structure decompositions at the zero lower bound. J. Appl. Economet. 33 (5), 643–661.
Christensen, J.H., Rudebusch, G.D., 2014. Estimating shadow-rate term structure models with near-zero yields. J. Financ. Econometet. 13 (2), 226–259.
Christensen, J.H., Rudebusch, G.D., 2016. Modeling yields at the zero lower bound: Are shadow rates the solution? In: Dynamic Factor Models. Emerald Group Publishing Limited, pp. 75–125.
Cogley, T., Sargent, T.J., 2008. Anticipated utility and rational expectations as approximations of bayesian decision making. Int. Econ. Rev. 49 (1), 185–221.
Dai, Q., Singleton, K.J., 2000. Specification analysis of affine term structure models. J. Finance 55, 1943–1978.
Dawachter, H., Iania, L., Wijnandts, J.-C., 2016. The response of euro area sovereign spreads to the ECB unconventional monetary policies. Technical Report. National Bank of Belgium.
Duffie, D., 1999. Credit swap valuation. Financ. Anal. J. 55 (1), 73–87.
Edwards, S., 1984. LDC foreign borrowing and default risk: An empirical investigation, 1976-80. Am. Econ. Rev. 74 (4), 726–734.
Egorov, A.V., Li, H., Ng, D., 2011. A tale of two yield curves: Modeling the joint term structure of dollar and euro interest rates. J. Econometet. 162 (1), 55–70.
Fontana, A., Scheicher, M., 2016. An analysis of euro area sovereign CDS and their relation with government bonds. J. Bank. Finance 62, 126–140.
Hamilton, J.D., Wu, J.C., 2012. Identification and estimation of Gaussian affine term structure models. J. Econometet. 168 (2), 315–331.
Hascoet, L., Pascual, V., 2013. The tapenade automatic differentiation tool: Principles, model, and specification. ACM Trans. Math. Softw. 39(3).
Ichiue, H., Ueno, Y., 2007. Equilibrium interest rate and the yield curve in a low interest rate environment. Bank Japan Discussion Paper No.07-E-18.
Kim, D.H., Priebsch, M., 2013. Estimation of multi-factor shadow-rate term structure models. Federal Reserve Board Discussion Paper Series.
Kim, D.H., Singleton, K.J., 2012. Term structure models and the zero bound: an empirical investigation of Japanese yields. J. Econometet. 170 (1), 32–49.
Kortela, T., 2016. A Shadow Rate Model with Time-Varying Lower Bound of Interest Rates. Bank of Finland Research Discussion Paper No. 19/2016.
Kreps, D.M., 1998. Anticipated utility and dynamic choice. Econ. Soc. Monogr. 29, 242–274.
Krippner, L., 2012. Modifying Gaussian term Structure Models when Interest Rates are Near the Zero Lower Bound, 2012/02. Reserve Bank of New Zealand Discussion Paper No. 2012/02.
Krippner, L., 2013. Measuring the stance of monetary policy in zero lower bound environments. Econ. Lett. 118 (1), 135–138.
Krippner, L., 2015. Zero Lower Bound Term Structure Modeling: A Practitioners Guide. Palgrave Macmillan.
Lemke, W., Vladu, A. L., 2017. Below the zero lower bound: A shadow-rate term structure model for the euro area. Working Paper Series - European Central Bank No. 1991/2017 1991.
Krippner, L., 2020. A note of caution on shadow rate estimates. J. Money Credit Bank. 52 (4), 951–962.
Liu, D.C., Nocedal, J., 1989. On the limited memory method for large scale optimization. Math. Programm. B 45(3), 503–528.
Manganelli, S., Wolswijk, G., 2009. What drives spreads in the euro area government bond market? Econ. Pol. 24 (58), 191–240.
Monfort, A., Renne, J.-P., 2013. Decomposing euro-area sovereign spreads: credit and liquidity risks. Rev. Finance 18 (6), 2103–2151.
Nelder, J.A., Mead, R., 1965. A simplex method for function minimization. Comput. J. 7, 308–313.
Orphanides, A., Wei, M., 2012. Evolving macroeconomic perceptions and the term structure of interest rates. J. Econ. Dyn. Control 36 (2), 239–254.
Pericoli, M., Taboga, M., 2015. Understanding policy rates at the zero lower bound: insights from a bayesian shadow rate model. Bank of Italy Temi di Discussione (Working Paper) No. 1023/2015 1023.
Ruge-Murcia, F.J., 2006. The expectations hypothesis of the term structure when interest rates are close to zero. J. Monet. Econ. 53 (7), 1409–1424.
Swanson, E.T., Williams, J.C., 2014. Measuring the effect of the zero lower bound on medium-and longer-term interest rates. Am. Econ. Rev. 104 (10), 3154–3185.
Swanson, E.T., Williams, J.C., 2014. Measuring the effect of the zero lower bound on yields and exchange rates in the UK and Germany. J. Int. Econ. 92, S2–S21.
White, H., 1982. Maximum likelihood estimation of misspecified models. Econometrica 50, 1–25.
Wu, J.C., Xia, F.D., 2016. Measuring the macroeconomic impact of monetary policy at the zero lower bound. J. Money Credit Bank. 48 (2-3), 253–291.
Wu, J.C., Xia, F.D., 2020. The negative interest rate policy and the yield curve. J. Appl. Econom. In press.